AD-A034 613 PHYSICS INTERNATIONAL CO SAN LEANDRO CALIF F/G 20/7
A FARADAY CUP WITH MULTIPLE INTERNAL FILTERS AND A PRIMARY CURR--ETC(U)
OCT 76 K CHILDERS, J SHEA F29601-75-C-0123
UNCLASSIFIED PIFR-835 AFWL-TR-76-132 NL

1 OF 1
AD-A
034 613

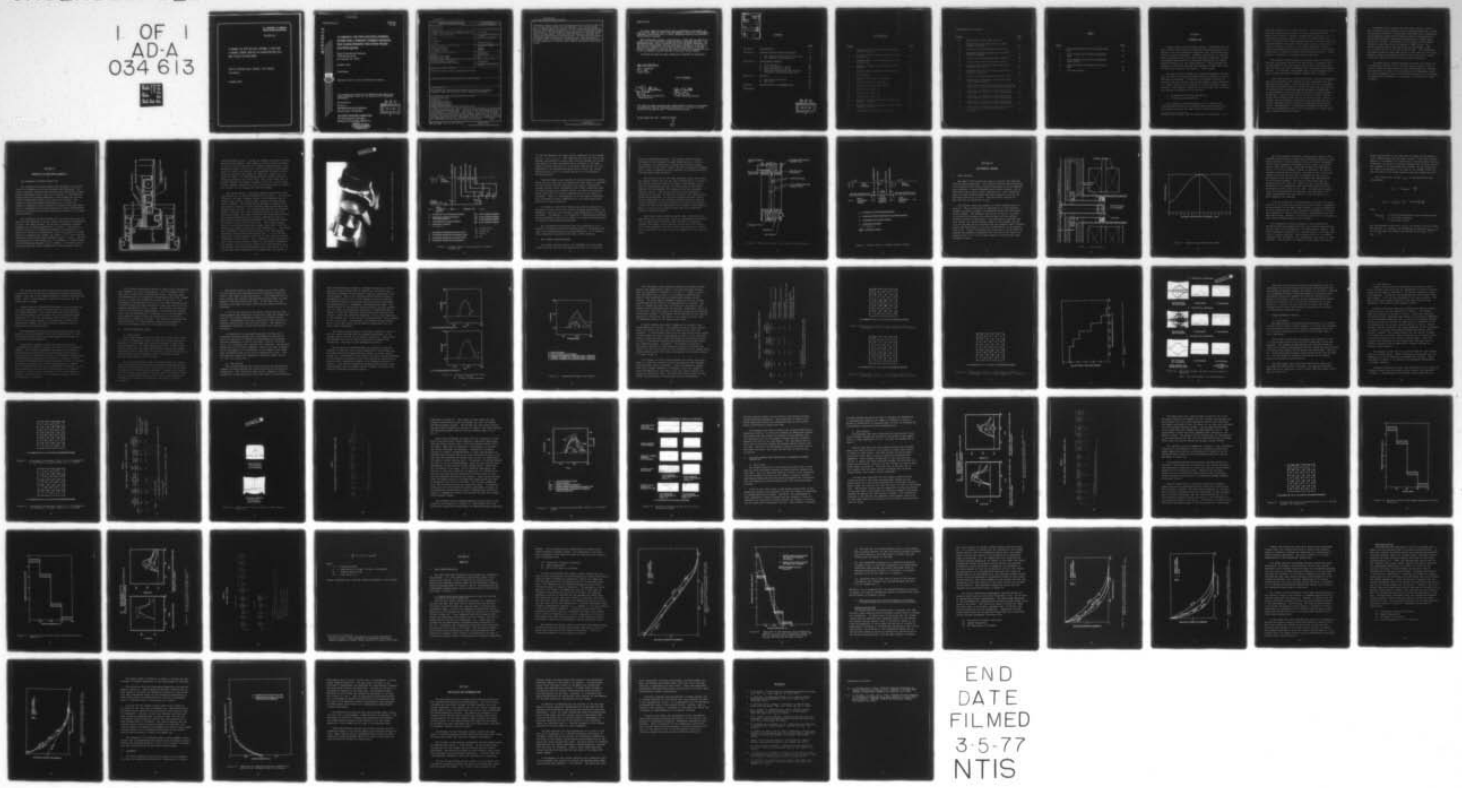

END
DATE
FILMED
3-5-77
NTIS

A FARADAY CUP WITH MULTIPLE INTERNAL FILTERS AND A PRIMARY CURRENT MONITOR FOR CHARACTERIZING HIGH DOSE PULSED ELECTRON BEAMS

PHYSICS INTERNATIONAL COMPANY, SAN LEANDRO
CALIFORNIA

OCTOBER 1976

AFWL-TR-76-132

AFWL-TR-
76-132

A FARADAY CUP WITH MULTIPLE INTERNAL FILTERS AND A PRIMARY CURRENT MONITOR FOR CHARACTERIZING HIGH DOSE PULSED ELECTRON BEAMS

Physics International Company
2700 Merced Street
San Leandro, CA 94577

October 1976

Final Report

This research was sponsored by the Defense Nuclear Agency under Subtask N99QAXAA121, Work Unit 10, Work Unit Title "Diagnostic Development".

Prepared for
Director
DEFENSE NUCLEAR AGENCY
Washington, DC 20305

AIR FORCE WEAPONS LABORATORY
Air Force Systems Command
Kirtland Air Force Base, NM 87117

UNCLASSIFIED

SECURITY CLASSIFICATION OF THIS PAGE *(When Data Entered)*

REPORT DOCUMENTATION PAGE		READ INSTRUCTIONS BEFORE COMPLETING FORM
1. REPORT NUMBER AFWL-TR-76-132	2. GOVT ACCESSION NO.	3. RECIPIENT'S CATALOG NUMBER
4. TITLE *(and Subtitle)* A FARADAY CUP WITH MULTIPLE INTERNAL FILTERS AND A PRIMARY CURRENT MONITOR FOR CHARACTERIZING HIGH DOSE PULSED ELECTRON BEAMS		5. TYPE OF REPORT & PERIOD COVERED Final Report 6. PERFORMING ORG. REPORT NUMBER PIFR-835
7. AUTHOR(s) K. Childers J. Shea		8. CONTRACT OR GRANT NUMBER(s) F29601-75-C-0123
9. PERFORMING ORGANIZATION NAME AND ADDRESS Physics International 2700 Merced Street San Leandro, CA 94577		10. PROGRAM ELEMENT, PROJECT, TASK AREA & WORK UNIT NUMBERS 62704H WDNA4003
11. CONTROLLING OFFICE NAME AND ADDRESS Director Defense Nuclear Agency Washington, D.C. 20305		12. REPORT DATE October 1976 13. NUMBER OF PAGES 76
14. MONITORING AGENCY NAME & ADDRESS*(if different from Controlling Office)* Air Force Weapons Laboratory Kirtland Air Force Base, NM 87117		15. SECURITY CLASS. *(of this report)* UNCLASSIFIED 15a. DECLASSIFICATION/DOWNGRADING SCHEDULE

16. DISTRIBUTION STATEMENT *(of this Report)*

Approved for public release; distribution unlimited.

17. DISTRIBUTION STATEMENT *(of the abstract entered in Block 20, if different from Report)*

18. SUPPLEMENTARY NOTES

This research was sponsored by the Defense Nuclear Agency under Subtask N99QAXAA121, Work Unit 10, Work Unit Title "Diagnostic Development".

19. KEY WORDS *(Continue on reverse side if necessary and identify by block number)*

Pulsed Electron Beams
Faraday Cup
Transverse Beam Energy
Energy Deposition Profile
Primary Current Monitor

20. ABSTRACT *(Continue on reverse side if necessary and identify by block number)*

A Faraday cup with multiple internal filters has been developed for characterizing intense pulsed electron beams. Four points on the charge deposition profile can be obtained on a single pulse. These data, in conjunction with the diode voltage histroy and Monte Carlo electron transport calculations, can be used to establish the average transverse beam energy (mean angle of incidence) and hence the energy deposition profile. Performance of the device was demonstrated for a 5kJ, 600keV beam that was transported from the diode using (over)

DD FORM 1 JAN 73 1473 EDITION OF 1 NOV 65 IS OBSOLETE

UNCLASSIFIED

SECURITY CLASSIFICATION OF THIS PAGE *(When Data Entered)*

longitudinal magnetic fields and that produced peak doses in excess of 200 cal/gm. A primary current monitor was also developed. This thin foil device, which is inserted between the diode and a target, measures the transported primary beam current passing through the foils, but not the low energy beam plasma return current. The present design caused attenuation of on the order of one-third of the beam energy. Three beam conditions obtained on the Model 225W Pulserad were characterized using these devices. The data confirm the absence of electron albedo in magnetically transported beams. Data obtained to investigate the effects of apertures on beam behavior indicate that apertures of 0.5-inch diameter or less lead to current waveforms that differ from the total current.

AFWL-TR-76-132

This final report was prepared by Physics International, San Leandro, CA, under Contract F29601-75-C-0123, Job Order WDNA4003, with the Air Force Weapons Laboratory, Kirtland AFB, NM. Lt. John A. MacFarlane (DYV) was the Laboratory Project Officer-in-Charge.

When US Government drawings, specifications, or other data are used for any purpose other than a definitely related Government procurement operation, the Government thereby incurs no responsibility nor any obligation whatsoever, and the fact that the Government may have formulated, furnished, or in any way by implication or otherwise as in any manner licensing the holder or any other person or corporation or conveying any rights or permission to manufacture, use, or sell any patented invention that may in any way be related thereto.

This technical report has been reviewed and is approved for publication.

JOHN A. MacFARLANE
1st Lt, USAF
Project Officer

FOR THE COMMANDER

CARL D. STUBER
Maj, USAF
Chief, Materials Vulnerability/
Hardening Branch

JOHN S. DeWITT
Lt Colonel, USAF
Chief, Technology Division

This report has been reviewed by the Information Office (OI) and is releasable to the National Technical Information Service (NTIS). At NTIS, it will be available to the general public, including foreign nations.

DO NOT RETURN THIS COPY. RETAIN OR DESTROY.

CONTENTS

ILLUSTRATIONS

ILLUSTRATIONS (Continued)

TABLES

SECTION I

INTRODUCTION

Intense pulsed electron beams provide a laboratory environment in which the pressure and impulse generating properties of materials and other phenomena associated with rapid energy deposition can be investigated. However, applications of electron beam environments for such studies have been frequently limited by problems associated with accurately determining the energy loading conditions in the target material. These problems are especially acute when the peak dose obtained exceeds the levels allowable for graphite calorimetry (~ 1200 cal/gm).

The goal of this program was to develop diagnostic devices that are useful at dose levels beyond those accessible with conventional calorimetry. Ultimately, one desires a device (or devices) that will measure the pulsed electron energy deposition in a target material as a function of lateral position, depth, and time. The specific objectives of this study were to develop and evaluate prototypes for two devices:

1. An Internally Filtered Faraday Cup
2. A Primary Current Monitor.

The internally filtered Faraday cup is a device that simultaneously measures the primary beam current deposited in the Faraday cup* and the beam current transmitted through a

*Conventional Faraday cups are described in References 1 to 6.

selected thickness of a filter material. This information, along with the accelerating voltage, is used in conjunction with Monte Carlo electron transport calculations (Reference 7) to determine the energy deposition profile in target materials. If such a device could be made sufficiently small, several internally filtered Faraday cups could then be used to obtain data on the lateral variation (if any) of the energy deposition profile. Since the Faraday cup provides time-resolved data, a full characterization of a beam environment would thus be possible. Consequently, a prototype of minimum size was desired.

The primary current monitor is a device that is inserted in the beam in between the anode and the target; it measures the primary beam current that passes through thin foils that intercept the beam, but does not measure the low energy plasma return current. It provides a measurement that can be related to the total energy (and hence, fluence) incident upon a target.

During the course of the investigation, limited experimental data were obtained on the effects of small apertures upon the measured beam currents. The results were such that it appeared that more extensive studies of these effects would be necessary to determine the minimum non-perturbing aperture dimensions. It was decided to avoid the aperture problem in this program by developing a large Faraday cup with several internal filters, rather than minimizing the size of the single filter version. A Faraday cup was therefore constructed that measured the total current deposited and the currents transmitted through three filters simultaneously. Considerable information relevant to the energy deposition profile can be obtained on a single diagnostic pulse with such a device.

Prototypes for a Faraday cup with three internal filters and a primary current monitor were developed successfully. These devices were evaluated in experiments performed with a magnetically transported pulsed electron beam on Physics International's Model 225W Pulserad; tests were conducted with a nominal beam voltage of 600 keV. Performance of the Faraday cup was demonstrated at peak dose levels in excess of 2000 cal/gm. The primary current monitor was generally not positioned in the most intense region of the beam in this study. Its performance was demonstrated for peak dose levels on the order of 1000 cal/gm. However, there are indications that it will function at levels where peak doses are greater than the 2000 cal/gm goal.

The experimental results obtained with both the Faraday cup with multiple internal filters and the primary current monitor clearly illustrate the merits of these new diagnostics. Moreover, the redundancy inherent in the combination of independent diode and beam diagnostics used in this study was found to be invaluable in determining the behavior of the beam in the diode and during transport.

SECTION II

ADVANCED ELECTRON BEAM DIAGNOSTICS

1. THE INTERNALLY FILTERED FARADAY CUP

The internally filtered Faraday cup developed in this program is an extension of existing Faraday cup technology. The (total stopping) collector was replaced with individually instrumented transmission foils, making it possible to simultaneously measure the total current deposited in the Faraday cup and the current transmitted through one or more thin filters. The purpose of the simultaneous measurements is to reduce the number of diagnostic pulses required to generate the data necessary to characterize an electron beam and to reduce experimental scatter in the data due to pulse-to-pulse variations in the beam characteristics.

The internally filtered Faraday cup initially had one filter but was later modified to contain three individually instrumented filters. The final version, the multiply internally filtered Faraday cup, is shown schematically in Figure 1. The body is similar to that of a conventional Faraday cup (Reference 3). A Mylar foil serves as a differential range filter and as a vacuum barrier to separate the Faraday cup vacuum ($< 10^{-3}$ torr) from the pressure in the electron beam transport region (1 torr). The current deposited in the Faraday cup is recorded as it flows around a self-integrating Rogowski coil to ground. An aluminum foil is used over the face of the Faraday cup to ensure proper feed of

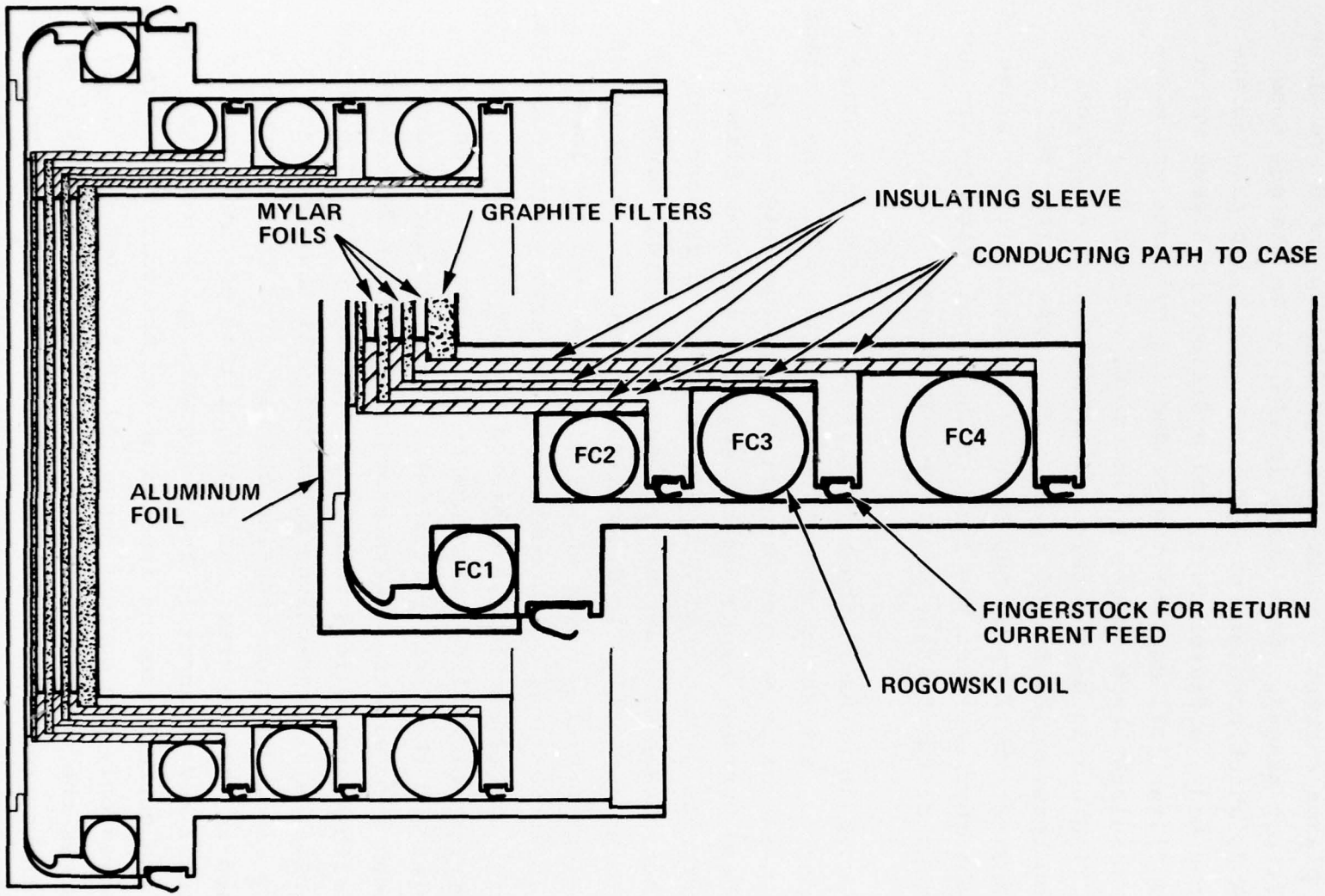

Figure 1 Schematic of Faraday cup with multiple internal filters.

the beam plasma current. Inside the Faraday cup there are three nesting filter stages. Each stage is similar to the one shown in Figure 2, which consists of a coaxial conducting path to the Faraday cup body, a filter foil, and a dielectric sleeve which holds the filter foil against the conducting cylinder and electrically insulates each stage; in addition, a Mylar foil not shown in Figure 2 is used between stages to assure electrical insulation between the filter foils. The first filter foil is pressed against the Faraday cup body by the first filter stage. A thick absorber replaces the foil in the final stage to protect the interior of the Faraday cup from beam damage.

The current paths in the beam transport region and inside the Faraday cup are shown schematically in Figure 3. The current flowing in the beam transport region is the algebraic sum of primary beam current, backscattered current, and beam plasma return currents. The Faraday cup is designed to measure only the energetic electron current (primary beam current minus the backscattered current). It discriminates between the energetic primary electrons, the lower energy electrons, and the low-penetrating-power ions which constitute the beam plasma currents. This energy discrimination is achieved through the use of a Mylar barrier which allows maintenance of a vacuum gap between the barrier and the first filter foil. Such a Mylar vacuum barrier can stop electrons with energies less than 20 keV and protons with energies less than 1 MeV (Reference 3). The vacuum gap establishes a space-charge potential well that prevents secondary electrons from crossing the gap. For the electron beams used in this program, the depth of this potential varied from about 2 keV to about 15 keV. Rogowski coils are sensitive only to the current flowing inboard of the monitor; therefore, FC4 measures only the current deposited in the beam stop (I_4), FC3 measures the current deposited in the third filter (I_3) as well as the current deposited in the beam stop (I_4) and so on

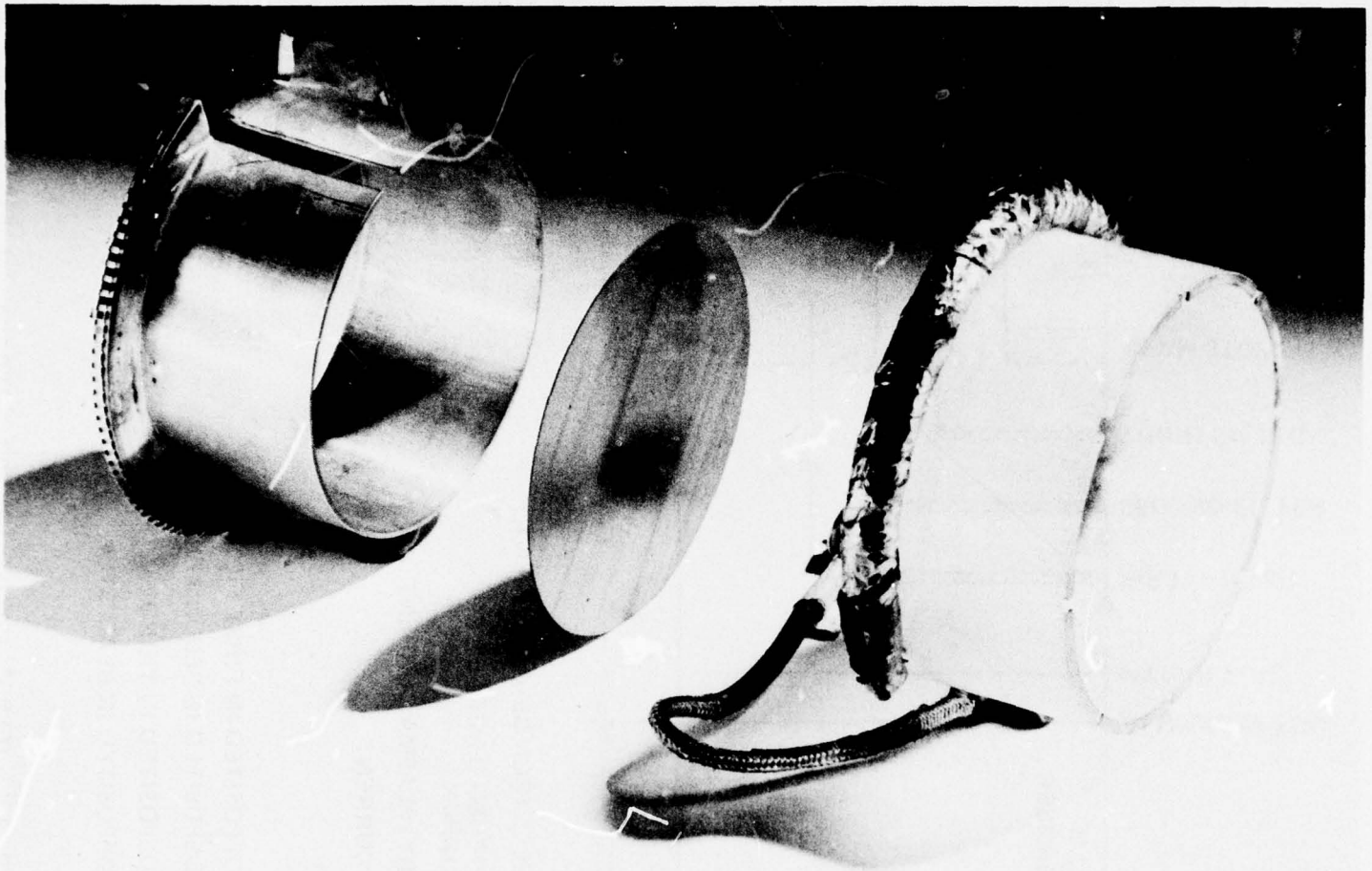

Figure 2 One stage of Multiply Internally Filtered Faraday Cup.

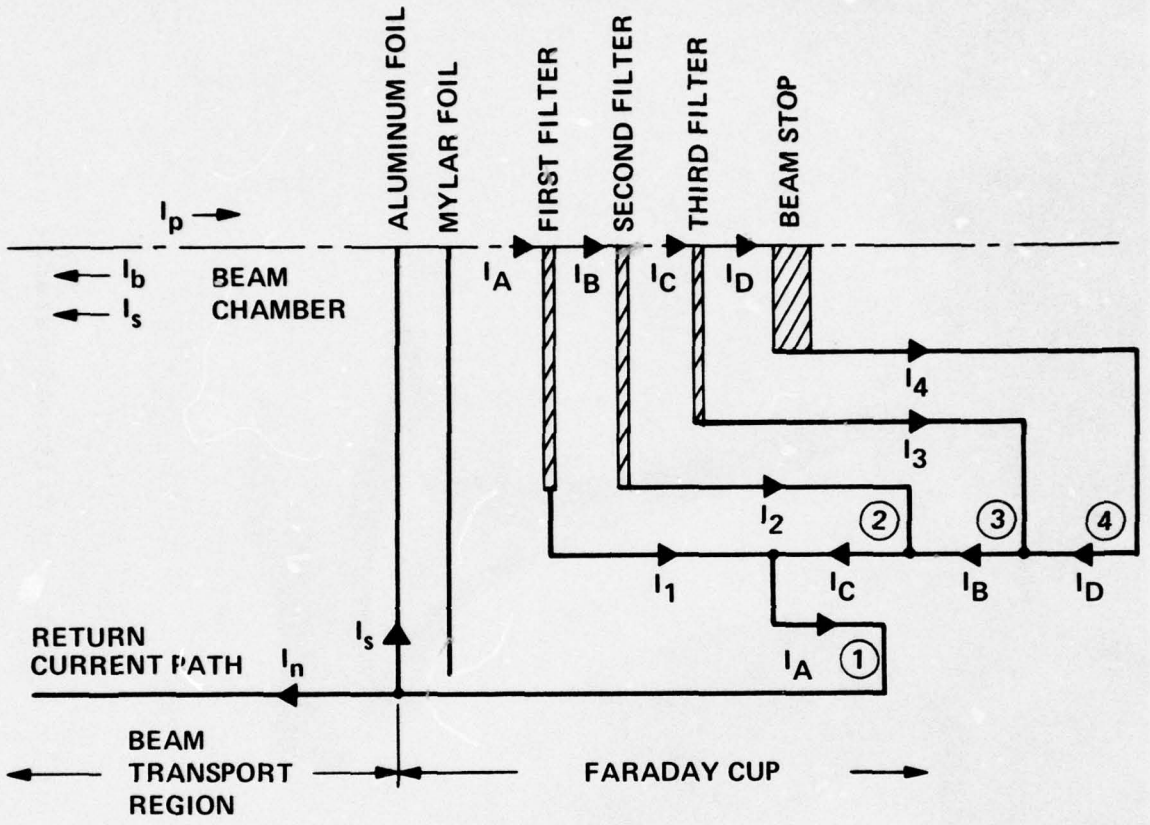

I_p IS PRIMARY ELECTRON BEAM CURRENT

I_b IS BACKSCATTERED (ENERGETIC) ELECTRON CURRENT

I_s IS (SECONDARY) PLASMA CURRENT

I_n IS BEAM NET CURRENT
$I_n = I_p - I_b - I_s$

I_1 IS CURRENT DEPOSITED IN FIRST FILTER

I_2 IS CURRENT DEPOSITED IN SECOND FILTER

I_3 IS CURRENT DEPOSITED IN THIRD FILTER

I_4 IS CURRENT DEPOSITED IN BEAM STOP

(1) IS FC1 CURRENT SENSOR

(2) IS FC2 CURRENT SENSOR

(3) IS FC3 CURRENT SENSOR

(4) IS FC4 CURRENT SENSOR

$I_A = I_1 + I_2 + I_3 + I_4$

$I_B = I_2 + I_3 + I_4$

$I_C = I_3 + I_4$

$I_D = I_4$

Figure 3 Current paths in the internally filtered Faraday cup.

so that FC1 measures the total current deposited in the Faraday cup ($I_1 + I_2 + I_3 + I_4$). The aluminum foil over the face of the Faraday cup provides a current path from the Faraday cup to the beam channel so that the plasma return currents in the beam channel can be properly fed. In practice some current will be deposited in the aluminum and Mylar foils so that the current measured by FC1 will be slightly smaller than the energetic electron current.

Filtered Faraday cups measure the charge deposition profile. These data are then used to determine the mean angle of incidence of the electron beam by correlating the current transmitted through various filter thicknesses with values calculated using the diode voltage and incident current (to obtain the electron energy spectrum) for various assumed values for the angle of incidence. Hence, a one-parameter fit to the data is obtained. This information permits computation of the energy deposition profile for target materials.

It should be noted that Faraday cups actually measure the deposited current and not the incident primary beam current; consequently, care must be exercised in how normalization of data is performed. Furthermore, it is difficult to differentiate between certain phenomena, such as the effect of transport efficiency and the effect of backscattered electrons.

The transmitted current data are time resolved so it is feasible to determine the time-resolved angle of incidence; however, time-resolved analysis is quite expensive, so in practice time-integrated correlations were used in this program.

2. THE PRIMARY CURRENT MONITOR

The primary current monitor is a Rogowski coil type beam current monitor that has been modified so that it is sensitive

only to primary beam current. The Primary Current Monitor developed in this program is shown schematically in Figure 4. It consists of a vacuum cavity defined by two Mylar vacuum barriers and a case which contains the self-integrating Rogowski coil; a pair of conducting foils adjacent to the Mylar barriers feed the beam plasma currents.

The current paths in the beam transport region and inside the primary current monitor are shown schematically in Figure 5. The current paths are similar to those in the Faraday cup in that the beam plasma currents are interrupted by the vacuum barriers and the Rogowski coil measures only the energetic electron current. The vacuum barriers can be separated if necessary to increase the potential well and thus increase the energy discrimination. As with the Faraday cup some current will be deposited in the aluminum and Mylar foils so that the incident energetic electron current will actually be slightly larger than the current measured by the primary current monitor, which in turn will be slightly larger than the transmitted energetic electron current.

The primary current monitor can be used to determine the beam fluence on a data pulse. This is accomplished by correlating the beam energy calculated from the diode acceleration voltage and primary current monitor current with beam energy and fluence measured at target location and using this correlation to determine the beam fluence on subsequent target irradiations.

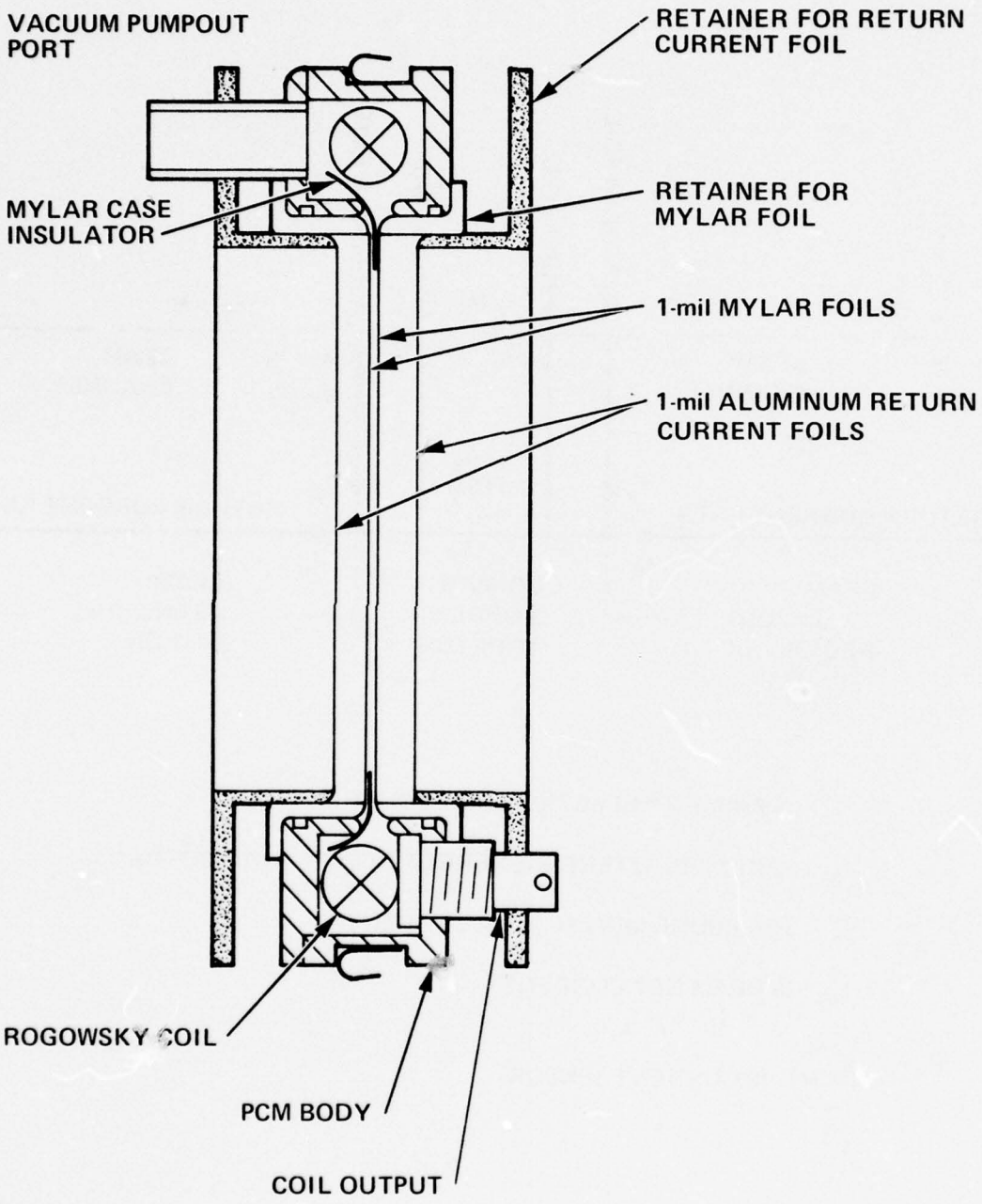

Figure 4 Schematic diagram of the primary current monitor.

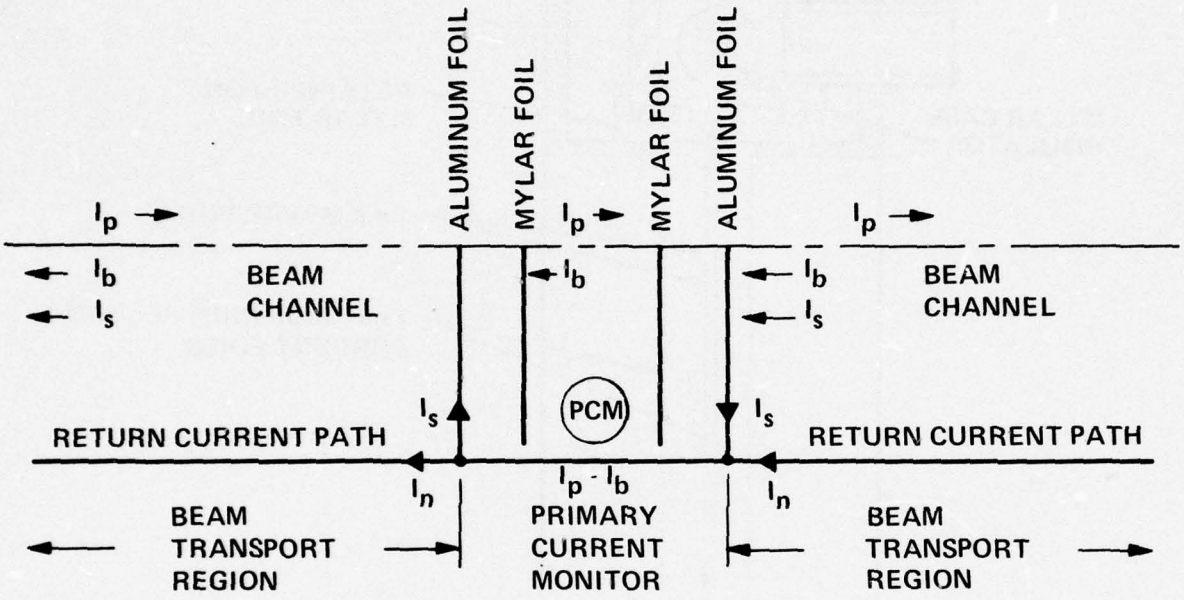

I_p IS PRIMARY ELECTRON BEAM CURRENT

I_b IS BACKSCATTERED (ENERGETIC) ELECTRON CURRENT

I_s IS (SECONDARY) PLASMA CURRENT

I_n IS BEAM NET CURRENT
$I_n = I_p - I_b - I_s$

(PCM) IS CURRENT SENSOR

Figure 5 Current paths in primary current monitor.

SECTION III

EXPERIMENTAL PROGRAM

1. TEST APPARATUS

The Model 225W Pulserad was used to evaluate the high-dose electron beam diagnostics. This pulsed electron beam accelerator is an advanced pulse charged system consisting of an oil-immersed Marx generator, a water-insulated pulse forming network, and an evacuated field emission diode (Reference 8). This system was used to obtain electron beams with mean energies up to 650 keV and beam energies up to 6½ kJ. The beam pulse duration on this facility is nominally 70 nsec.

The electron beam test geometry is shown schematically in Figure 6. The electron beam is generated by a field emission cathode and passes through a transmission anode into the experimental chamber. The magnetic lens shown in Figure 7 was used to control and transport the electron beam from the cathode emission surface to the target. This produces an electron beam that retains the cross-sectional shape of the cathode, but the area of the beam varies inversely with the magnetic field strength; hence, the beam fluence is directly proportional to the magnetic lens ratio. Fluence uniformity was controlled to first order by dishing the cathode to compensate for the bow of the anode produced by the 1 torr (130 Pa) gas pressure in the electron beam transport region.

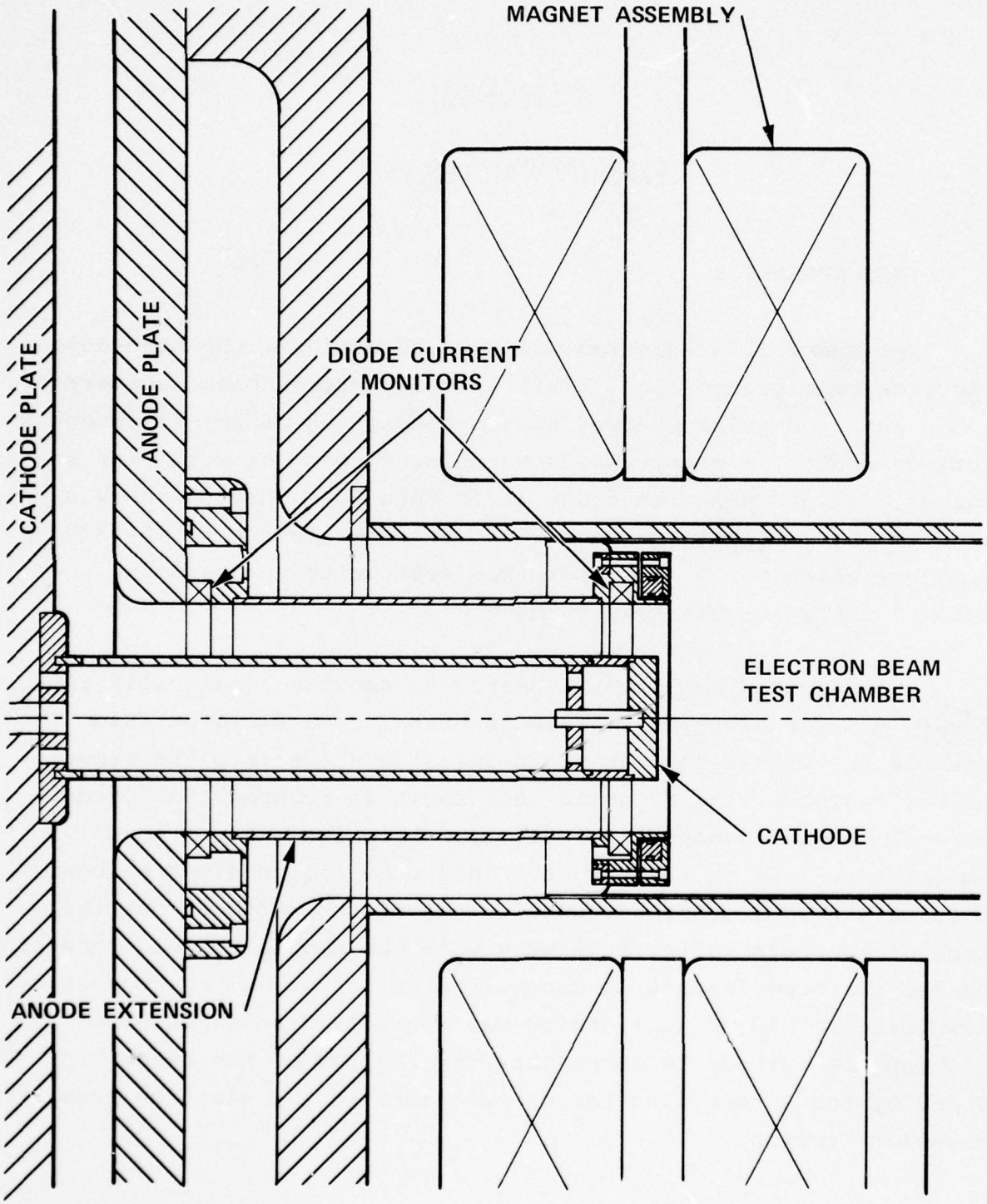

Figure 6 Test geometry.

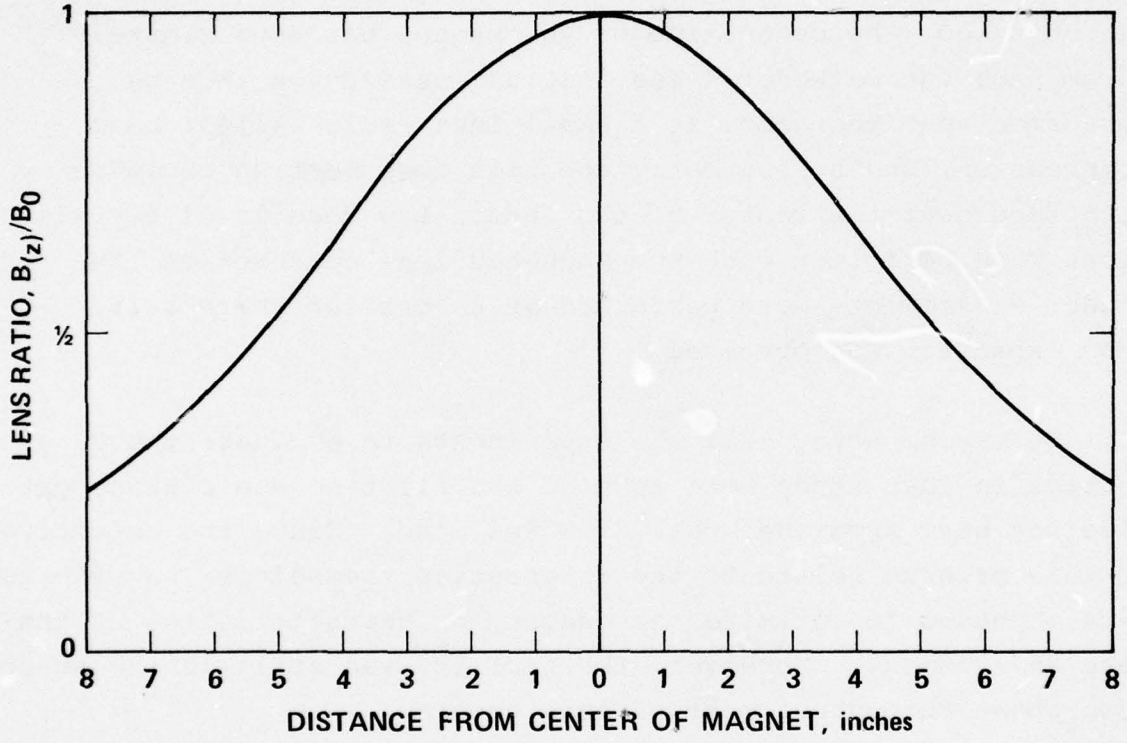

Figure 7 Magnetic beam guide field shape.

The diode and beam transport configurations used for this program were designed to obtain beam environments where the peak doses achieved in target materials could be varied from modest levels (where graphite calorimeters can be used) up to levels greater than 2000 cal/gm. The diode geometry was designed to use a 5 cm (2 inch) diameter cathode to generate a 60 cal/cm^2 (nominal) beam of 500 to 600 keV. For most of the testing the magnet was positioned such that a maximum lens ratio of 4:1 was obtained (the centerline of the magnet was approximately 20 cm from the cathode). The initial tests could thus be performed near the anode at a small lens ratio (slight beam compression) and subsequently the high dose testing could be performed near the center of the lens. Low dose level correlations were performed with the magnetic lens centered on the anode; experiments were performed at a location where a 2:1 beam expansion was obtained.

It may be noted that the experiments to evaluate the diagnostics in this study were some of the first to use a transported electron beam from the Model 225W Pulserad. Since the objectives of this program relate to the diagnostics themselves, no efforts were expended to optimize the quality or characteristics of the beam environment. Moreover, the facility was still in the shakedown phase throughout most of this program.

The diagnostic devices developed in this program were evaluated based upon comparisons with the electron beam monitors for the diode and calorimeters in the experimental chamber. The diode diagnostics consisted of a voltage monitor, a $\dot{B}$ probe, and a set of current monitors. The voltage monitor is a resistive voltage divider attached to the transmission line near the diode insulator. The $\dot{B}$ probe is a magnetic field sensor that has an

output proportional to the time rate of change of the magnetic field ($\dot{B}$) associated with the diode current. Each diode current monitor is a Rogowski coil consisting of a $\dot{B}$ probe with a built-in integrator; the output is directly proportional to diode current. The Rogowski coils surrounded the cathode: one was located in the anode plate adjacent to the base of the cathode stalk (I0) and the other in the anode extension near the cathode tip (I1).

The acceleration voltage, V_{acc}, is determined from the relationship:

$$V_{acc} = V_{monitor} - L \frac{dI}{dt}$$

or

$$V_{acc} = V_{monitor} - \left(L \times \text{constant}\right) \times \frac{dB}{dt}$$

where

$V_{monitor}$ is the voltage measured by the voltage monitor
L is the diode inductance
I is the diode current

and the constant is the ratio I/B at the location of the $\dot{B}$ probe. The product, L x constant, is determined by comparing $V_{monitor}$ to the $\dot{B}$ probe when the cathode was shorted to the anode (i.e., $V_{acc} = 0$).

The voltage monitor and $\dot{B}$ signals were electronically subtracted after the $\dot{B}$ signal was suitably attenuated and properly phased to provide a null combined signal on shorted anode-cathode shots. Thus, it was possible to obtain on-line data for the acceleration voltage.

Signals from the diagnostics developed in this program and the diode diagnostics were recorded with fast oscilloscopes ($\geq$ 150-MHz bandwidth). The oscilloscope data were digitized and fed into Physics International (PI) data processing codes (Reference 9). The data processing codes correct the input data for L/R slumps inherent in the monitors, determine the acceleration voltage, and then calculate parameters used to characterize the electron beam.

The acceleration voltage and current waveforms were used directly in the PIEID Monte Carlo Code (Reference 10) to calculate electron beam energy and charge deposition profiles for correlation with measurements.

Conventional graphite fluence and deposition profile calorimeters were used to diagnose the beam in the experimental chamber. The fluence calorimeters consisted of ATJ graphite blocks that were mounted on fiberglass boards with aluminum screws which were instrumented with iron-constantan thermocouples. The thermocouple signals were recorded by a scanning digital voltmeter that sampled each probe approximately every 1¼ seconds. The thermal equilibration time was approximately 10 seconds and the thermal decay time was approximately 200 seconds, so the peak thermocouple readings were deemed adequate to determine fluences. Fluences were calculated with a PI mini-computer program, using polynomial fits to handbook enthalpy curves for ATJ graphite and aluminum.

The electron beam energy deposition profile was investigated with graphite foil stack calorimeters. The ATJ graphite foils were held in position by polyethylene blocks. The foils were instrumented with iron-constantan thermocouples that were clamped against a copper tab attached to an edge of each foil. The thermocouple signals were read out with the same scanning digital voltmeter system described previously, except that each foil was sampled approximately every ½ second. The thermal equilibration time for the foils were approximately 4 seconds and the thermal decay time was approximately 50 seconds, so it was necessary to plot thermal response curves and extrapolate to zero-time to determine the deposition profiles. The deposition profiles were calculated with a PI mini-computer program using polynomial fits to the enthalpy curves for ATJ graphite and copper.

2. INITIAL FEASIBILITY TESTS

a. Test Design

The primary objective of the first test series was to check out the new diagnostics, namely to find out if they functioned properly or to determine what might be necessary to make them function properly. The main concerns were that (1) the current sensors should have the same sensitivity at operational levels (hundreds of kA) as they have at the levels at which calibrations are performed (tens of amperes), and (2) that they measure primary beam current, not net current.

Once the monitors were shown to function properly, quantitative evaluation could then begin by checking them against one another and comparing them with calorimetry at dose levels where calorimetry can be used with confidence. An additional concern for the primary current monitor was the effect the monitor might have on the transmitted beam; in the initial test sequence experiments were planned to investigate its effect on fluence uniformity.

The initial tests on the new Faraday cup and the primary current monitor were conducted with each diagnostic placed as close to the anode as was practicable. It was expected that at this location the fluence levels would be sufficiently low that graphite calorimeters could be used. At the same time, any changes in the beam that might occur during transport would be minimized.

In the initial design of the primary current monitor the vacuum pumpout was positioned in such a way that the Faraday cup could not be located immediately behind the primary current monitor. Consequently, data were obtained for each monitor on separate pulses during the first test series. The design was subsequently modified to allow both devices to be used concurrently.

In preparation for developing multiple (minimum size) internally filtered Faraday cups, experiments to explore the effect of apertures on Faraday cup measurements were planned. Aperture diameters of 0.32 cm (1/8-inch), 0.64 cm (1/4-inch), and 1.3 cm (1/2-inch) were selected for evaluation. The aperture plates were 0.25 cm thick graphite. This is the same thickness as the collimator (1.3 cm aperture) on the graphite foil depth dose calorimeter used in the initial experimental tests. Thus the apertures tested had diameter to thickness aspect ratios of 1.25, 2.5, and 5.0 to 1.

b. Test Results

The current monitors were initially tested by shorting the cathode to ground through the current monitors and pulsing the accelerator. This forced the same current, nominally 120 kA, through all of the monitors so that they could be intercalibrated.

The intercalibration procedure, performed routinely at the beginning of each pulsing series, checked out the entire data acquisition system, current sensors, cabling, attenuators, and oscilloscopes. One of the intercalibration pulses revealed a manufacturing flaw in one of the Faraday cup current sensors. The defective sensor was replaced and satisfactory performance was demonstrated on a subsequent intercalibration pulse. The current sensor in the primary current monitor initially checked out, but after two pulses the sensitivity increased by about a factor of three and thereafter demonstrated some waveform distortion. Post-test inspection revealed a flaw in the insulation of the Rogowski coil of the primary current monitor, which allowed an arc to the case. Consequently, the primary current monitor data in this test series can be used for qualitative but not quantitative information.

The primary current monitor functioned properly in that it gave an output waveform that was roughly proportional to the primary current and not to net current (Figure 8). Arcing from the Rogowski coil to the case of the monitor disrupted the integration, resulting in some waveform distortion.

The internally filtered Faraday cup appeared to function properly in that the total current deposited in the Faraday cup was qualitatively and quantitatively similar to diode current (Figure 9). Furthermore, diode current and total current deposited in the Faraday cup varied by only a few percent in amplitude and shape so that transmitted current can be compared directly in Figure 9. The current transmitted through various filter thickness decreases with increasing filter thickness indicating that internal filtering functions properly.

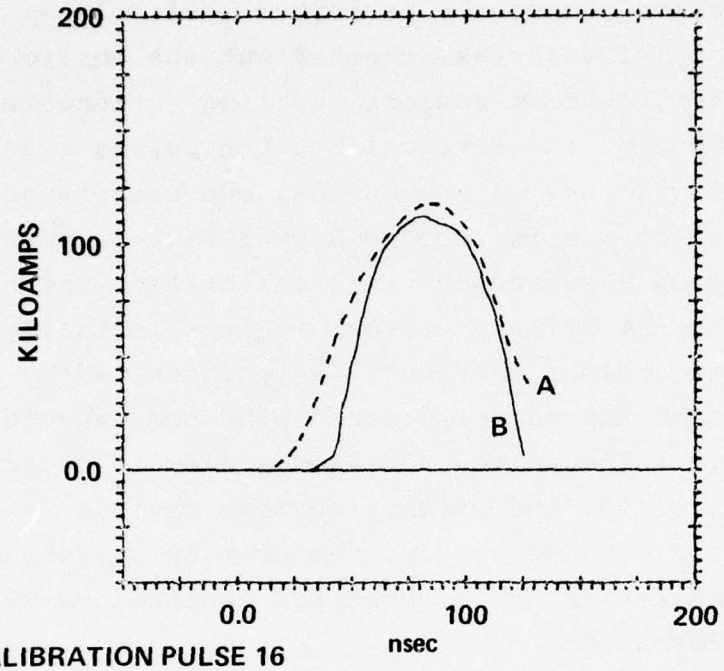

A. INTERCALIBRATION PULSE 16

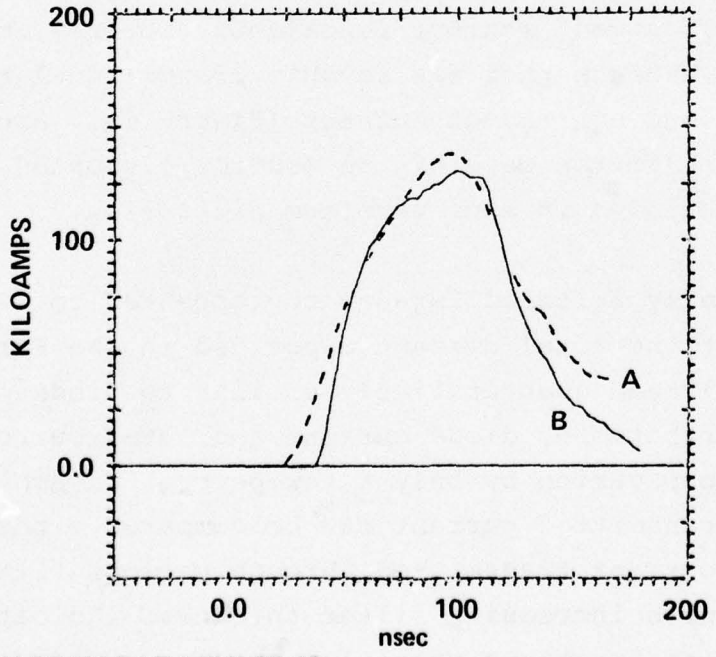

B. ELECTRON BEAM DATA PULSE 18

Figure 8 Primary current monitor data.
a. Diode current.
b. Primary current monitor.

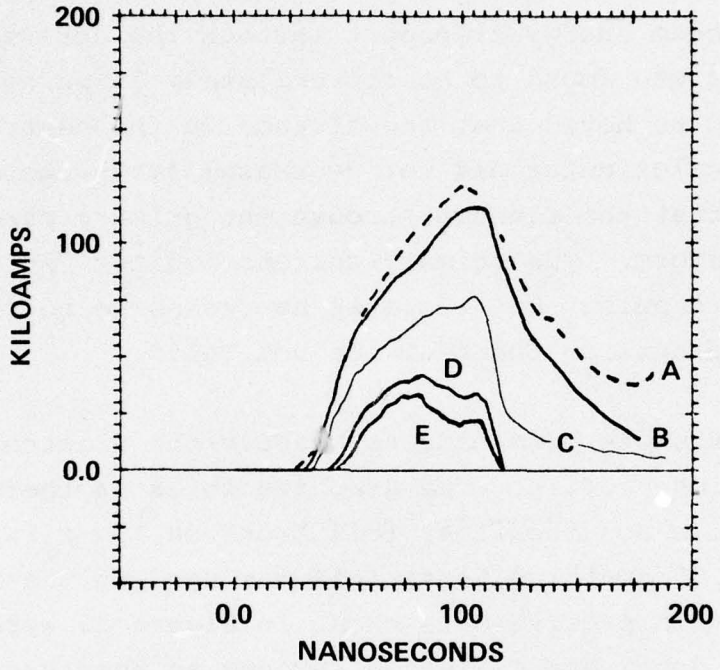

A–DIODE CURRENT
B–TOTAL FARADAY CUP CURRENT
C–CURRENT TRANSMITTED THROUGH 0.015 in. GRAPHITE
D–CURRENT TRANSMITTED THROUGH 0.025 in. GRAPHITE
E–CURRENT TRANSMITTED THROUGH 0.030 in. GRAPHITE

Figure 9 Transmitted Faraday cup current.

The calorimeter data collected through the primary current monitor are summarized in Table 1, and the individual fluence maps are presented in Figures 10, 11, and 12. Pulses 31 and 32 were performed with no foils in the primary current monitor; pulse 35 was performed with an operational primary current monitor. The beam energy transport through the active primary current monitor was found to be approximately 75 percent. However, it should be noted that the fluence in the central nine probes of the calorimeter did not decrease; furthermore, there is an indication that the fluence through the primary current monitor may be more uniform. The primary current monitor did not function properly on this pulse, but there is no reason to believe that the observed effects on the beam are not valid.

Several attempts were made to measure the electron beam energy deposition profile. The graphite foils in these calorimeters are fragile and the first foil broke on the first two attempts. A 0.05-cm-thick first foil was used on the final attempt and the deposition profile data shown in Figure 13 were obtained. However, these data were collected through an aperture identical to the 1.3-cm-diameter aperture discussed below which may affect the transmitted beam. In addition, the fluence indicated by the energy deposited in the deposition profile calorimeter was found to be 30 cal/cm^2 which is only 55 percent of the (unapertured) fluence measured with the fluence calorimeter in the same location on Pulses 31 and 32.

The Faraday cup data obtained behind the various apertures, shown in Figure 14, display serious discrepancies when compared with the diode current waveforms. These discrepancies suggest that either larger diameter to thickness ratios are needed to avoid perturbation of the beam or that the current density distribution varies with time. The data also cause concern for the design characteristics of deposition profile calorimeters.

TABLE 1

INITIAL FEASIBILITY TESTING CALORIMETER DATA

Pulse	Peak[1] Acceleration Voltage (kV)	Peak[1] Diode Current (kA)	Average Fluence (cal/cm^2)	Energy Deposited in Calorimeter[3] (kJ)	Comment
31	690	100	$55 \pm .8$[2]	4.5	Fluence calorimeter No foils in primary current monitor
32	670	97	54 ± 9[2]	4.4	Fluence calorimeter No foils in primary current monitor
35	680	102	56 ± 4[2]	3.4	Fluence calorimeter Primary current monitor active (no data)
40	690	110	30	0.16	Deposition profile calorimeter, 1.3-cm-diameter aperture No foils in primary current monitor

NOTES:
1. Oscilloscope data
2. Determined from central 9 calorimeter probes ± MSD
3. Calorimeter directly behind primary current monitor

1	2 22	3 46	4 52	5 4
6 21	7 71	8 49	9 54	10 58
11 44	12 55	13	14 51	15 77
16 39	17 59	18	19 45	20 75
21 4	22 62	23 78	24 60	25 28

5 x 5 ARRAY OF 1 cm x 1 cm x 0.79 cm ATJ GRAPHITE BLOCKS

Figure 10 Fluence map, Pulse 31; total energy deposited in calorimeter, 4.5 kJ; average fluence 55 ± 8 cal/cm^2.

1	2 30	3 49	4 38	5 55
6 28	7 67	8 46	9 56	10 67
11 38	12 51	13	14 44	15 77
16 46	17 66	18	19 46	20 69
21 3	22 52	23 75	24 47	25 24

5 x 5 ARRAY OF 1 cm x 1 cm x 0.79 cm ATJ GRAPHITE BLOCKS

Figure 11 Fluence map, Pulse 32; total energy deposited in calorimeter, 4.4 kJ; average fluence, 54 ± 9 cal/cm^2.

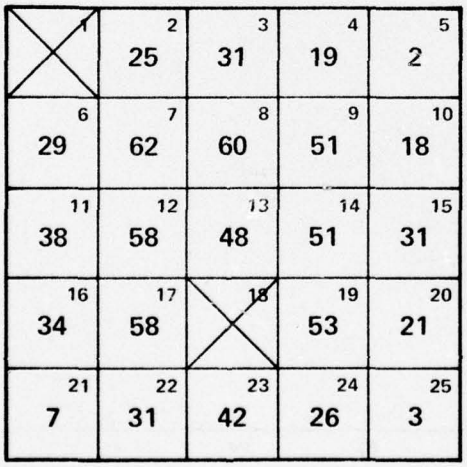

5 x 5 ARRAY OF 1 cm x 1 cm x 0.79 cm ATJ GRAPHITE BLOCKS

Figure 12 Fluence map, Pulse 35; total energy deposited in calorimeter, 3.4 kJ; average fluence, 56 ± 4 cal/cm^2.

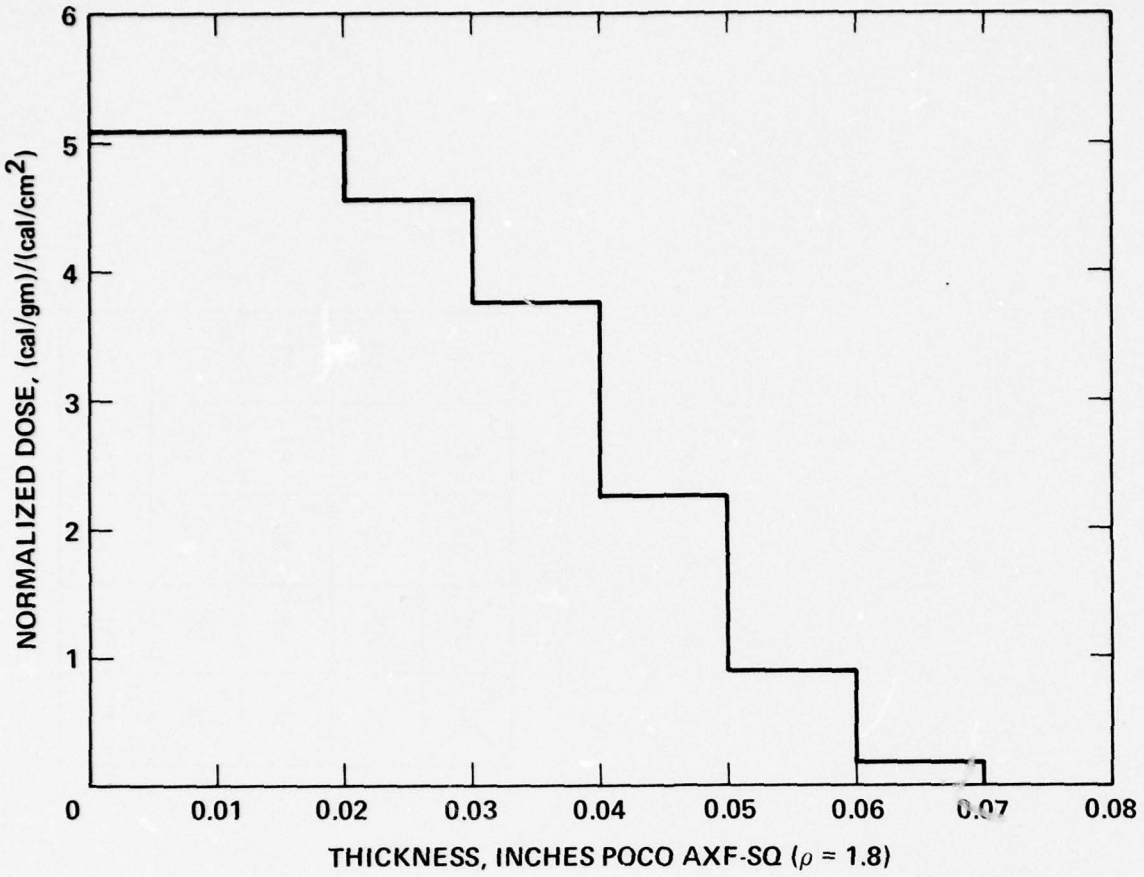

Figure 13 Measured electron beam energy deposition profile, Pulse 40.

A. PULSE 37 (½-in. APERTURE)

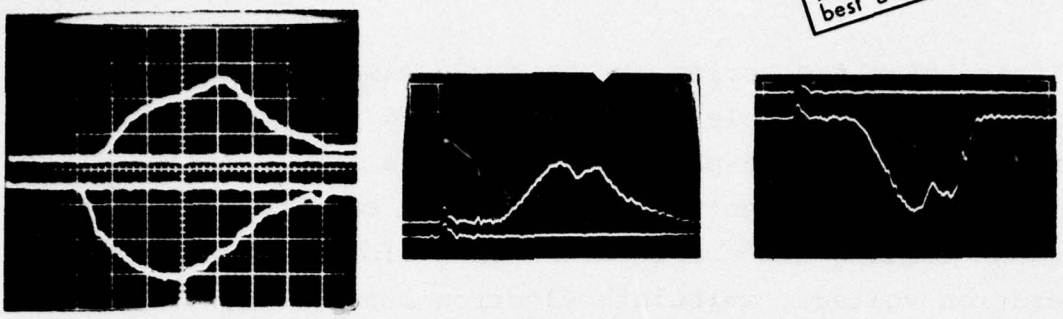

50 kA/DIVISION
256 kV/DIVISION

5 kA/DIVISION

2.7 kA/DIVISION

B. PULSE 39 (¼-in. APERTURE)

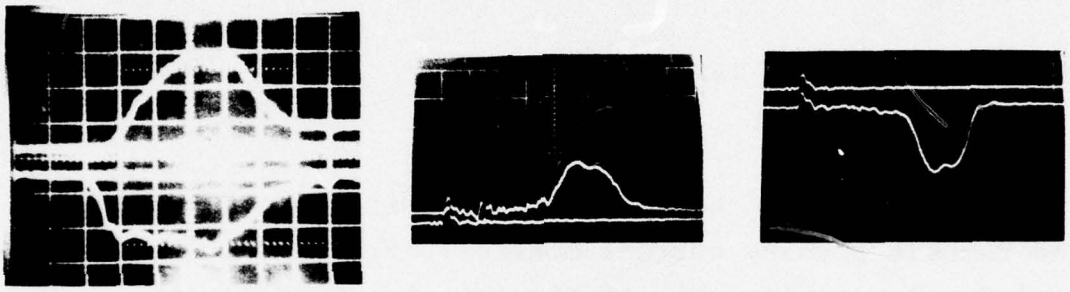

50 kA/DIVISION
256 kV/DIVISION

5 kA/DIVISION

2.7 kA/DIVISION

C. PULSE 38 (1/8-in. APERTURE)

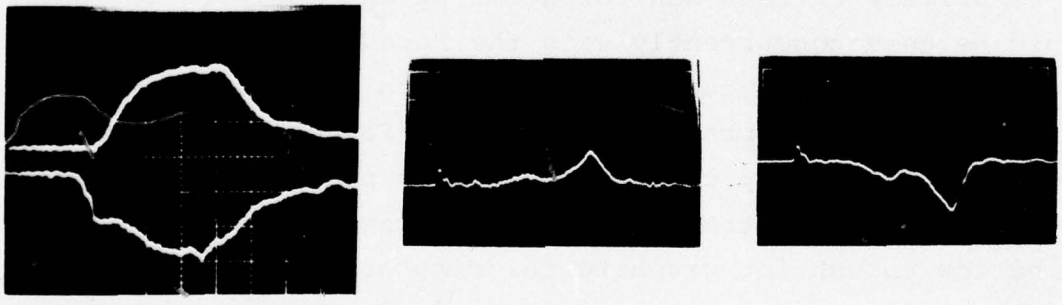

50 kA/DIVISION
256 kV/DIVISION

DIODE CURRENT AND
CORRECTED VOLTAGE

1.2 kA/DIVISION

FC 1

0.7 kA/DIVISION

FC 2 WITH
0.015-in. GRAPHITE
FILTER

Figure 14 Apertured Faraday cup data, 0.038 cm thick Ta aperture.

Note: All sweep speeds = 20 nsec/division.

After this test series an error was discovered in the determination of the acceleration voltage and some difficulty was experienced in properly phasing the signals for analysis. Although it is possible to correct these data based on information from subsequent testing and complete the analysis (calculate the acceleration voltage, calculate electron beam energy and charge deposition profiles, etc.), it was not considered to be cost effective. Instead care was exercised to assure that these problems did not recur and analytical resources were expended in understanding subsequent data.

3. FINAL FEASIBILITY TESTING

a. Test Design

The objectives of the second test series were (1) to check-out the rebuilt primary current monitor, (2) to use the internally filtered Faraday cup to collect current transmission data, and (3) to further investigate the effect of using higher aspect ratio aperatures.

The primary current monitor geometry was modified so that it could be used concurrently with the Faraday cup in this test sequence. The primary current monitor then was positioned as close to the anode as practicable and the Faraday cup was positioned as close to the primary current monitor as practicable. This was done to minimize beam transport difficulties and so that the dose would be low enough for graphite calorimeters to be useable behind the preimary current monitor.

The high aspect ratio apertures selected for these tests were made of 0.038-cm-thick tantalum. The aperture diameters were 0.64 cm (¼ inch) and 1.3 cm (½ inch); thus the aspect ratios were 17 and 33 to 1.

b. Test Results

Primary current monitor performance was initially erratic until the Mylar case insulator was implemented to prevent internal arcing in the monitor; thereafter, the monitor appeared to function properly. The monitor was assembled with the minimum vacuum gap, namely ~ 0.013 cm, the thickness of the case insulator. The Mylar foils were pressed together in the beam channel by the pressure in the electron beam transport region.

Fluence calorimetry data were collected through the primary current monitor, and are summarized in Table 2. The fluence maps are presented in Figures 15 and 16. These data show that 91 percent of the (computed) beam energy in the diode is deposited in the calorimeter when there are no foils in the primary current monitor, but only 67 percent of diode energy is deposited in the calorimeter when the primary current monitor is active. Consequently, the data show that the energy deposited in the calorimeter is reduced 25 percent by transport through the primary current monitor. However, the average fluence for the central 9 probes is reduced only 10 percent (after adjusting for 10 percent difference in beam energy in the diode on those pulses). This fact coupled with inspection of the fluence maps indicates that the fluence uniformity may be improved by transport through the primary current monitor.

The Faraday cup was used as a target holder for the calorimeter in the above tests. Since there was no vacuum barrier, the Rogowski coil in the Faraday cup recorded net currents. These are shown in Figure 17 to contrast with subsequent measurements of primary currents.

Selected transmitted current data obtained with the internally filtered Faraday cup and primary current monitor are summarized in Table 3. Representative voltage and current waveforms are

1 0	2 13	3 53		5 2
6 10	7 72	8 60	9 66	10 43
11 21	12 81	13 48	14 61	15 66
16 6	17 75	18 64	19 71	20 43
21 1	22 11	23 51	24 38	25 4

5 x 5 ARRAY OF 1 cm x 1 cm x 0.79 cm ATJ GRAPHITE BLOCKS

Figure 15 Calorimeter fluence map, Pulse 55; 4.0 kJ deposited in calorimeter; average fluence, 66 ± 9 cal/cm^2.

1 1	2 15	3 32		5 3
6 7	7 47	8 39	9 56	10 16
11 13	12 57	13 50	14 60	15 26
16 7	17 50	18 66	19 58	20 18
21 1	22 5	23 15	24 9	25 2

5 x 5 ARRAY OF 1 cm x 1 cm x 0.79 cm ATJ GRAPHITE BLOCKS

Figure 16 Calorimeter fluence map, Pulse 57; 2.7 kJ deposited in calorimeter; average fluence, 55 ± 6 cal/cm^2.

TABLE 2

FINAL FEASIBILITY TESTING CALORIMETER DATA

Pulse	Peak[1] Acceleration Voltage (kV)	Peak[1] Diode Current (kA)	Peak[1] Primary Current Monitor Current (kA)	Peak[2] Net Current (kA)	Diode[3] Energy (kJ)	Average[4] Fluence cal/cm^2	Energy Deposited in Calorimeter (kJ)	Comment
55	650	120		9.5	4.4	66 ± 9	4.0	No foils in primary current monitor
57	640	130	110	2.7	4.0	55 ± 6	2.7	Primary current monitor active

NOTES:

1. Oscilloscope data
2. Measured with Faraday cup, which was used as target holder, oscilloscope data
3. $\int V_{ACC} \times I_{DIODE}\, dt$
4. Determined from central nine calorimeter probes, ± MSD

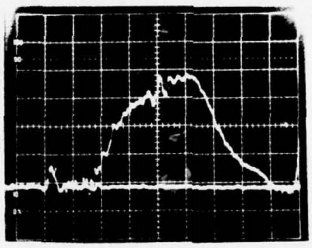

DIODE CURRENT
32 kA/DIVISION
20 nsec/DIVISION

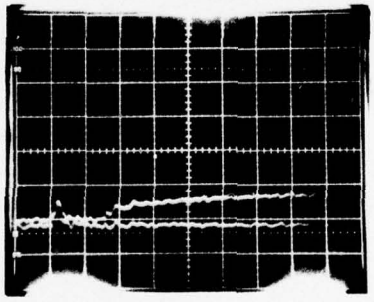

BEAM NET CURRENT
14 kA/DIVISION
20 nsec/DIVISION

Figure 17 Diode current and net current in beam channel, Pulse 55.

TABLE 3

FINAL FEASIBILITY TESTING TRANSMITTED CURRENT DATA

Pulse	Peak[1] Acceleration Voltage (kV)	Peak Diode Current (kA)	Charge[2] in Diode (mC)	Peak[1] Primary Current Monitor Current (kA)	Transmitted Charge[2] Through Primary Current Monitor (mC)	Peak Current[1] Deposited in Faraday Cup (kA)	Charge[2] Deposited in Faraday Cup (mC)	----Internal Filter---- Graphite Filter[3] Thickness ($\rho = 1.76$) (10^{-3} cm)	Transmitted[2] Charge (mC)	Comment
60	670	130	9.9	105	8.0	105	7.3	8 ± 1	5.3 ± 0.2	
61	610	130	9.4	100	7.6	100	7.0	20 ± 1	3.8	
62	640	140	9.7	110	8.2	100	6.8	38 ± 1	2.7 ± 0.3	
63	650	140	9.7	110	8.2	110	7.3	51 ± 1	2.1 ± 0.2	

NOTES:
1. Oscilloscope data
2. $\int I\,dt$, error bars reflect truncation errors (and errors associated with reading small signals)
3. Error bars reflect actual uncertainty and uncertainty associated with porosity of filter

presented in Figure 18. This figure clearly shows that the primary current monitor and the Faraday cup (FC1) are indeed recording primary current. The Faraday cup and primary current monitor current records are similar to those of the diode current, and differed markedly from net current records shown in Figure 17.

The current waveforms in Figure 18 also illustrate a difficulty that occurs with current monitors; they often break away from the actual current into a long time constant decay late in the pulse. When this is observed it is necessary to truncate the current waveforms for analysis. Truncation of primary currents is usually straightforward; a linear extrapolation is effected from the point where the decay initiates to zero at the time that the acceleration voltage goes to zero (at which point the primary current must be zero). Truncation of filtered Faraday cup data is not as straightforward, since the zero current point corresponds to some non-zero diode voltage value. These data were truncated in two ways: by (1) abruptly terminating the current at the first indication of decay and (2) extending the decay to the time that the acceleration voltage goes to zero and then abruptly terminating the current. These values provide lower and upper limits on the deposited charge which were used to establish error bars on the data. For the data presented here, the truncation errors are relatively small. It should be noted that the intercalibration pulses, performed routinely at the beginning of each pulsing series, substantially reduce the errors in transmitted current data because the data are treated using relative values.

The Faraday cup data obtained behind the high aspect ratio apertures are presented in Figure 19. Much smaller but still significant qualitative differences are observed between apertured

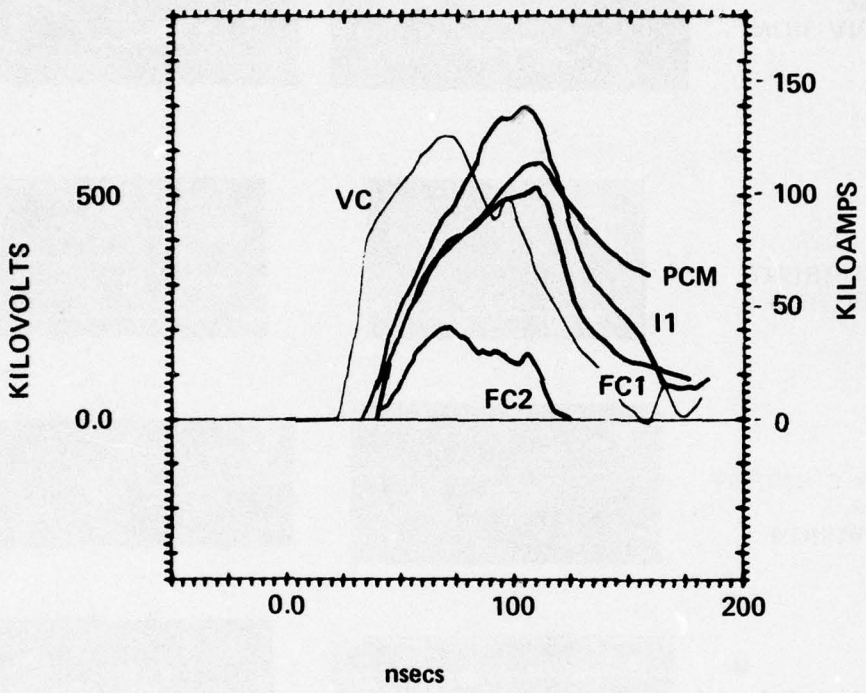

VC = ACCELERATION VOLTAGE
I1 = DIODE CURRENT
PCM = PRIMARY CURRENT MONITOR
FC1 = BEAM CURRENT DEPOSITED IN FARADAY CUP
FC2 = BEAM CURRENT TRANSMITTED THROUGH 0.02-INCH GRAPHITE

Figure 18 Voltage and current waveforms, Pulse 63, 60 cal/cm^2 level.

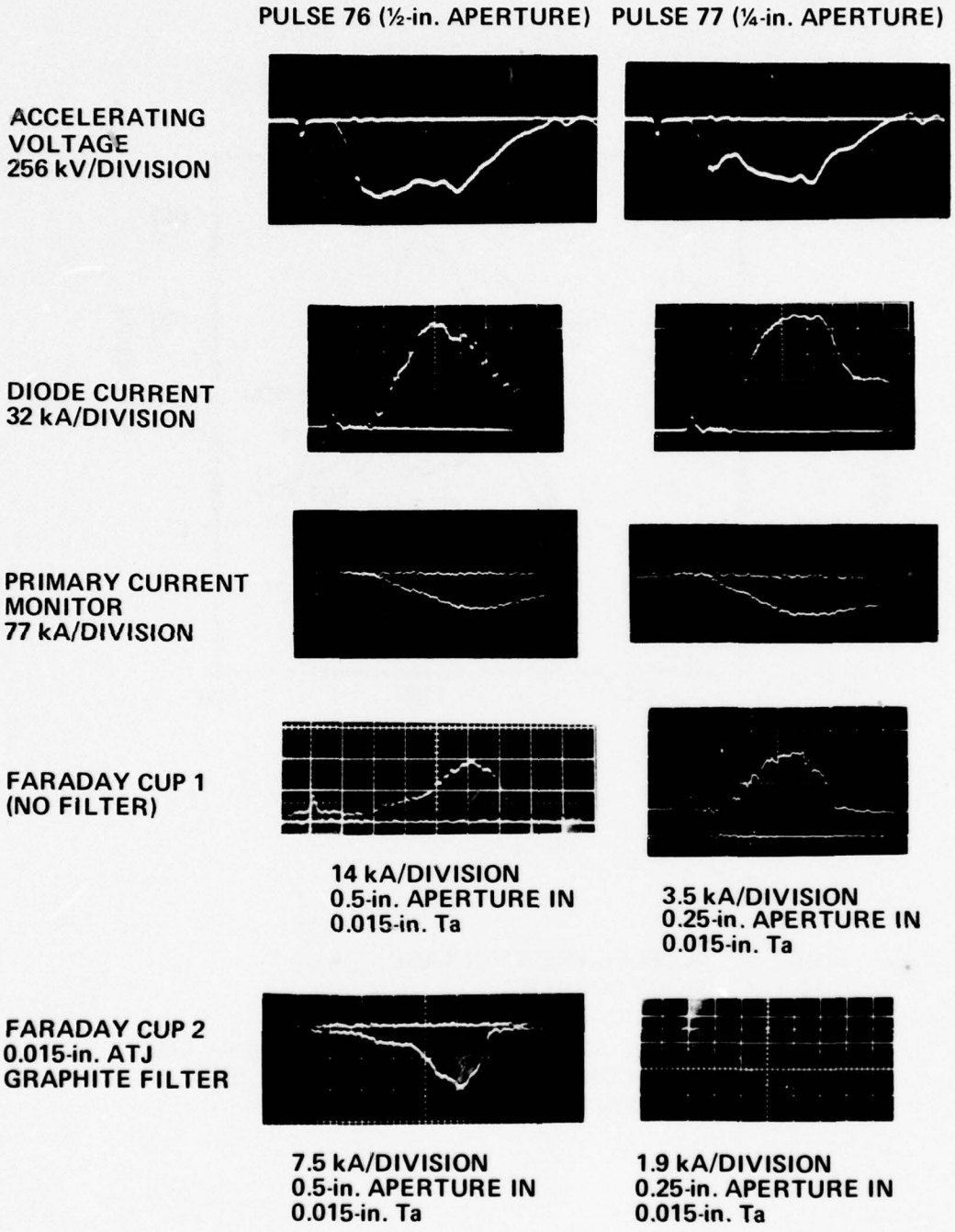

Figure 19 Apertured Faraday cup data 0.25 cm thick graphite aperture.

currents and the primary current monitor and between currents through different apertures. This continues to suggest that either apertures perturb the transported beam or the current density distribution varies with time.

Two attempts were made to measure the electron beam energy deposition profile. On the first attempt the deposition profile calorimeter was used behind the primary current monitor, but the vaporized foils in the primarly current monitor evidently smashed the foils in the calorimeter. The calorimeter was re-built and on the final attempt the primary current monitor was not used. The foils in the deposition profile survived, but no data were retrieved. The cause for the loss of data was not discovered.

4. HIGH DOSE TESTING WITH THE MULTIPLY INTERNALLY FILTERED FARADAY CUP

a. Test Design

The primary objective of the third test series was to show that the newly developed diagnostics would function properly at high dose. The two additional internal filters in the internally filtered Faraday cup would also be tested. Finally, electron beam energy deposition profiles would be measured for correlation with the deposition profiles deduced from the filtered Faraday cup data.

Prior to this test series it had become obvious that it was beyond the scope of this program to pursue the effects of apertures on transported electron beams. Therefore, the development of small internally filtered Faraday cups was dropped in favor of extending the internally filtered Faraday cup concept to include the two additional instrumented filters. This multiply internally

filtered Faraday cup would be used to evaluate the feasibility of substantially reducing the number of diagnostic pulses required to characterize an electron beam, as well as relaxing the requirements on pulse-to-pulse reproducibility.

b. Test Results

The high-dose data were collected with the multiply internally filtered Faraday cup located in the center of the magnet lens at a beam compression of 4:1. The data are summarized in Table 4.

During these tests the pulse charge voltage was increased above that used previously in an effort to ensure dose levels in excess of 2000 cal/gm. The beam voltage was maintained at levels near those used in earlier testing by reducing diode impedance. These changes caused some of the electron beam current to impact the anode extension between the anode and the diode current monitor, resulting in the voltage and current waveforms shown in Figure 20. This data set is the only one in this program that had diode current waveforms that differed significantly from primary current waveforms.

The data were obtained with the primary current monitor placed as close to the anode as practicable except for one pulse (pulse 212), which was performed with the primary current monitor near the focus of the lens (directly in front of the Faraday cup). The primary current monitor apparently functioned properly at the high dose on this pulse, but the beam transport efficiency through the monitor was significantly reduced. The transmitted currents in the Faraday cup appeared to have deeper penetration on this pulse than on the pulses with the primary current monitor near the anode.

VC ACCELERATION VOLTAGE
I1 DIODE CURRENT
FC1 BEAM CURRENT DEPOSITED IN FARADAY CUP
FC2-FC4 TRANSMITTED CURRENTS

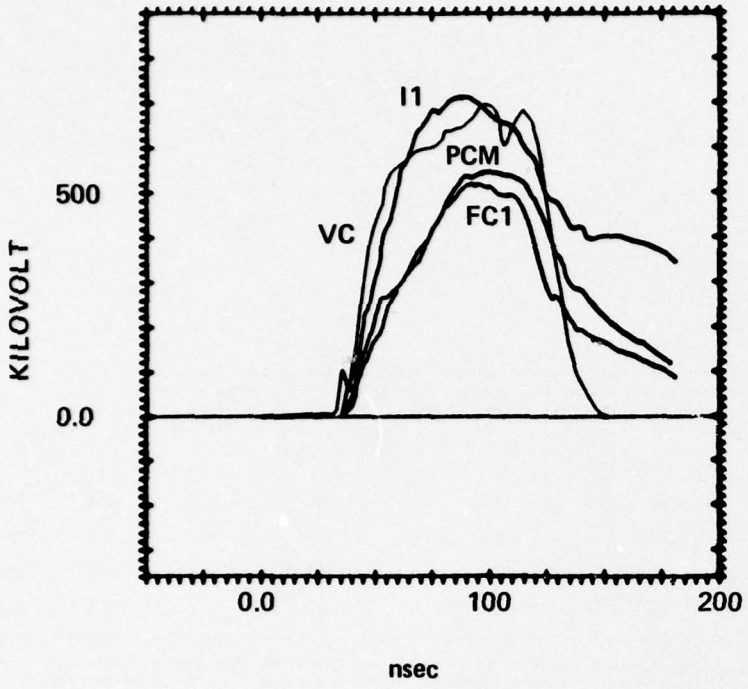

DIODE VOLTAGE, DIODE CURRENT, PCM CURRENT, AND FARADAY CUP CURRENT

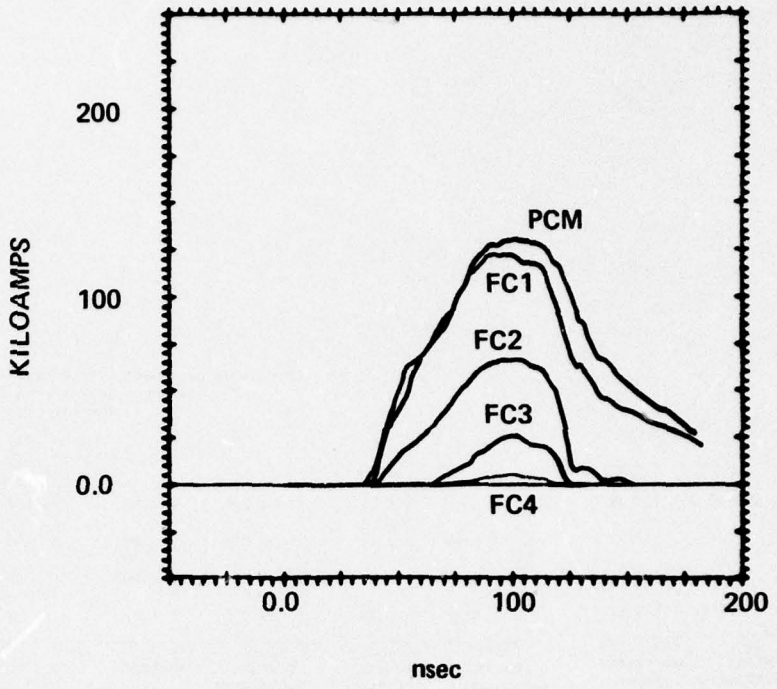

PCM CURRENT, AND FARADAY CUP INCIDENT AND TRANSMITTED CURRENTS

Figure 20 Voltage and current waveforms, pulse 222, 4:1 beam compression 225 cal/cm^2 level.

TABLE 4

HIGH DOSE TESTING TRANSMITTED CURRENT DATA

Pulse	Peak[1] Acceleration Voltage (kV)	Peak[1] Diode Current (kA)	Peak[1] Primary Current Monitor Current (kA)	Charge[2] Transmitted Through Primary Current Monitor (mC)	Peak[1] Current Deposited in Faraday Cup (kA)	Charge[2] Deposited in Faraday Cup (mC)	First Filter Stage		Second Filter Stage		Third Filter Stage	
							Graphite[3] Filter Thickness (10^{-3} cm)	Transmitted[2] Charge (mC)	Graphite[3] Filter Thickness (10^{-3} cm)	Transmitted[2] Charge (mC)	Graphite[3] Filter Thickness (10^{-3} cm)	Transmitted[2] Charge (mC)
214	670	170	130	8.9	120	7.4	33 ± 1	3.5 ± 0.4	33 ± 1	0.82 ± 0.03	33 ± 1	0.08 ± 0.02
219	680	160	130	10.0	130	8.8	51 ± 1	2.3 ± 0.5	51 ± 1	0.2 ± 0.2	∞	--
221	670	170	---[4]	(9.0 ± 0.5)[4]	120	7.8	51 ± 1	1.9 ± 0.2	51 ± 1	0.07 ± 0.07	∞	--
222	700	170	130	9.4	120	8.4 ± 0.1	33 ± 1	3.9 ± 0.1	33 ± 1	0.9	33 ± 1	0.15 ± 0.02

NOTES:
1. Oscilloscope data
2. $\int I\,dt$ error bars reflect truncation errors and errors in measuring small signals
3. Error bars reflect actual uncertainties and uncertainties associated with filter porosity
4. Primary current monitor malfunctioned, estimate based on correlation with charge deposited in Faraday cup

The magnet position, which had been fixed for all of the preceding testing, was changed for the low dose testing when the correlations with the energy deposition profile were obtained. The magnet was moved so that the center of the lens was coincident with the cathode emission surface. The testing was performed at 5½-inches from the cathode with beam expansion of 2:1. The pulse-charge voltage and diode impedance were returned to the nominal values. The primary current monitor was not used because it was anticipated that the thin foil deposition profile calorimeters would not survive behind the primary current monitor.

The low-dose data are summarized in Table 5. The calorimeter fluence map is presented in Figure 21; measured electron beam energy deposition profiles are presented in Figures 22 and 23. Representative voltage and current waveforms for this testing are shown in Figure 24.

The agreement between diode current and beam current deposited in the Faraday cup is remarkable; the current waveforms are essentially identical up to the time that the diode current breaks into an exponential decay. However, the late-time behavior of the transmitted current monitors gave relatively large truncation uncertainties in transmitted charges compared to earlier results.

Several unsuccessful attempts were made with different deposition profile calorimeters before deposition profile data were obtained. However, the beam energy deposited in the deposition profile calorimeter was only about half of that measured with a fluence calorimeter that was positioned behind a 1-1/8 inch diameter graphite aperture identical to the collimator on the deposition profile calorimeter. Furthermore, the beam fluence calculated from beam energy in the diode using the relationship

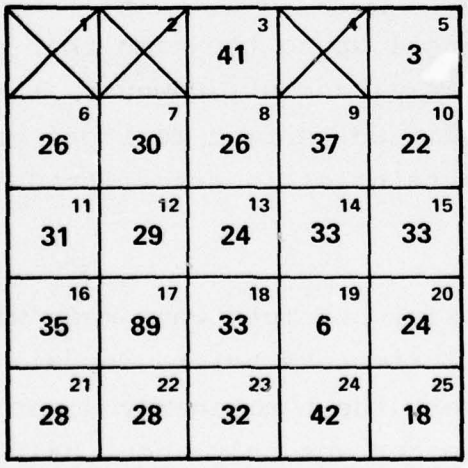

5 x 5 ARRAY OF 1 cm x 1 cm x 0.79 cm ATJ GRAPHITE BLOCKS

Figure 21 Fluence map Pulse 232 average fluence, 31 ± 6 cal/cm^2 through 2.9 cm aperture.

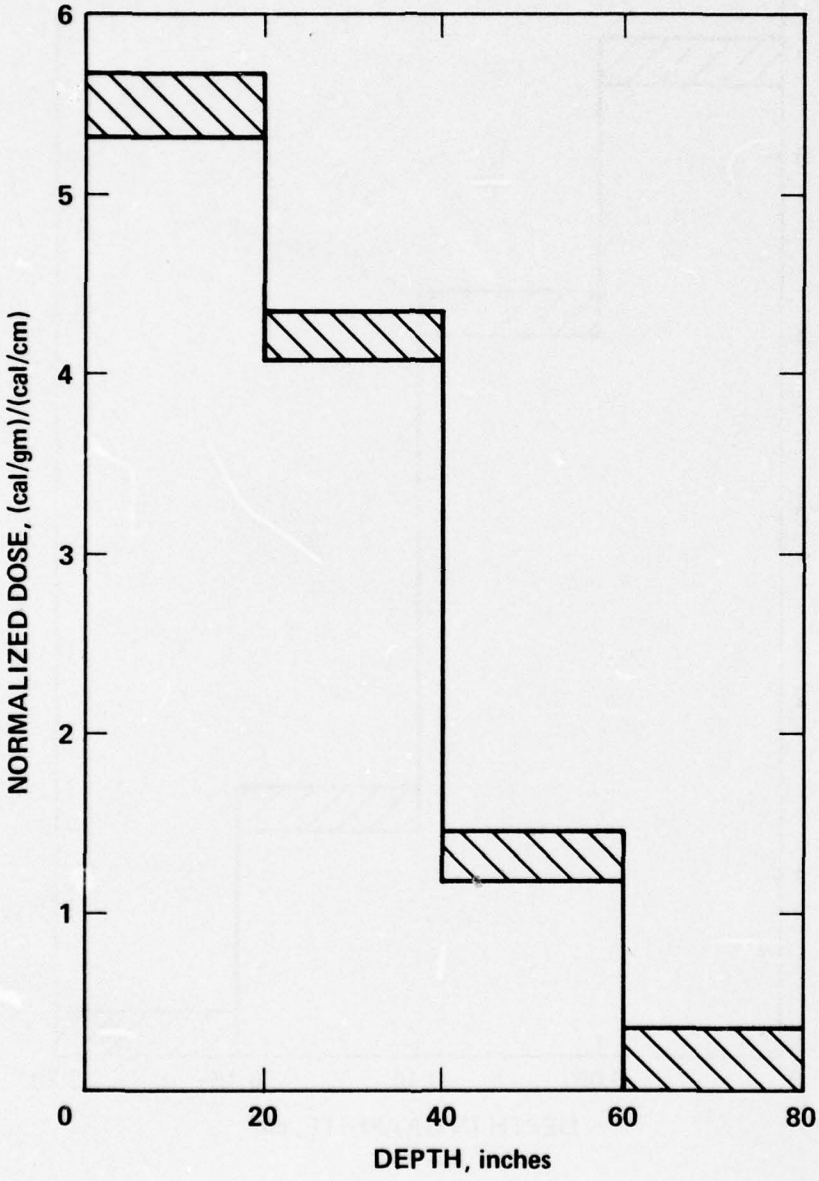

Figure 22 Measured electron beam energy deposition profile, Pulse 239.

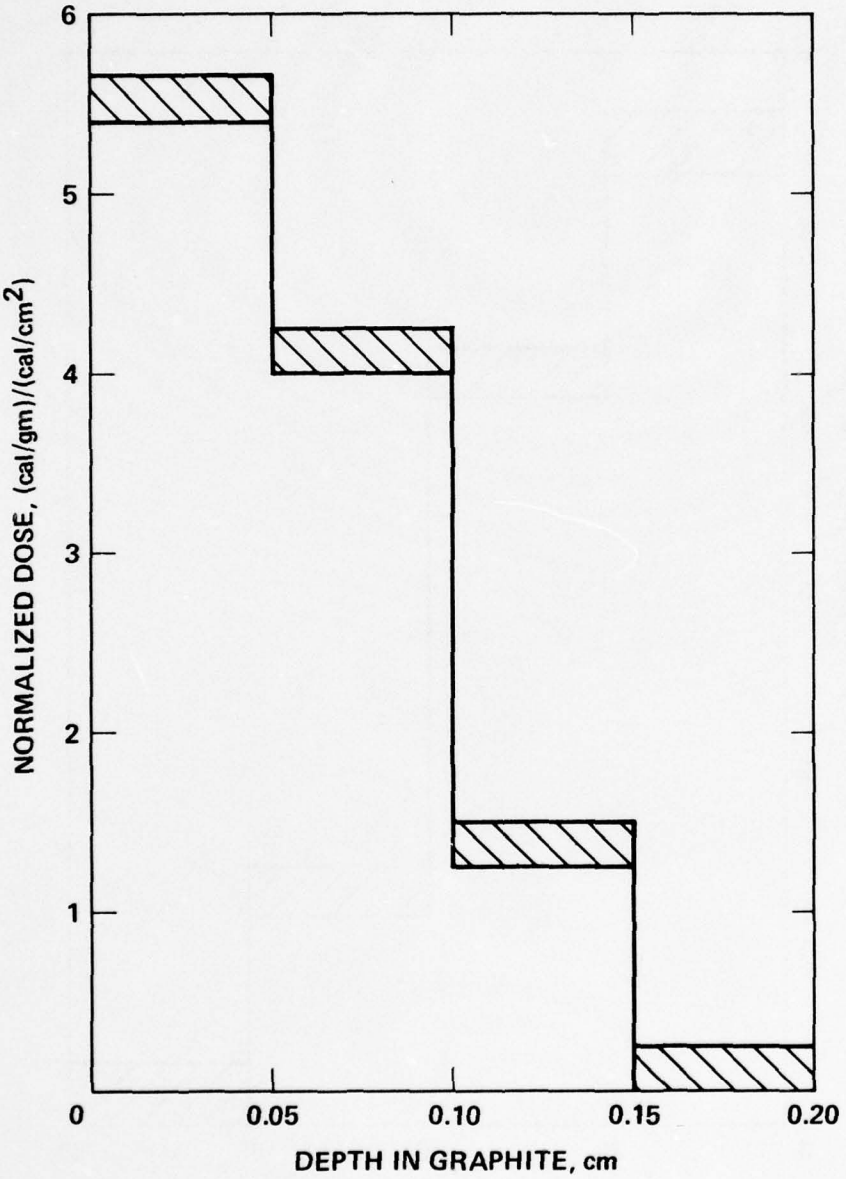

Figure 23 Measured electron beam energy deposition profile, Pulse 247.

VC ACCELERATION VOLTAGE
I1 DIODE CURRENT
FC1 BEAM CURRENT DEPOSITED IN FARADAY CUP
FC2-FC4 TRANSMITTED CURRENTS

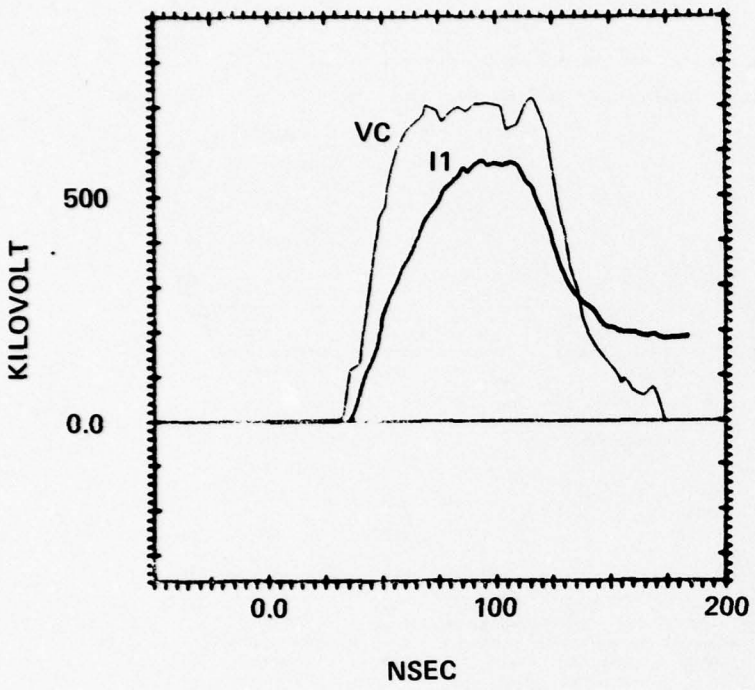

DIODE VOLTAGE AND CURRENT

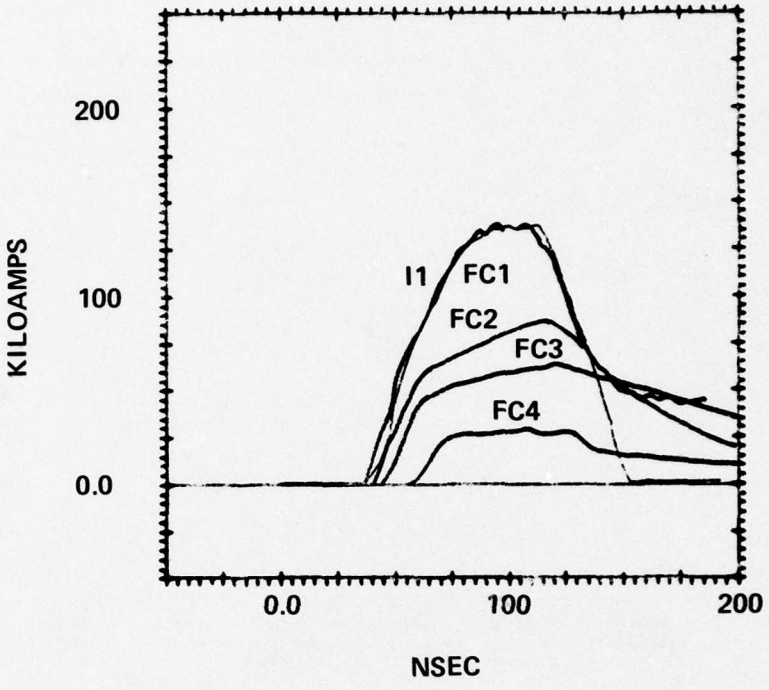

DIODE CURRENT AND FARADAY CUP INCIDENT AND TRANSMITTED CURRENTS

Figure 24 Voltage and current waveforms, pulse 231, 2:1 beam expansion 30 cal/cm^2 level.

TABLE 5

LOW DOSE TESTING

a. Transmitted Charge Data

Pulse	Peak[1] Acceleration Voltage (kV)	Peak[1] Diode Current (kA)	Charge[2] in Diode (mC)	Peak[1] Current Deposited in Faraday Cup (kA)	Charge[2] Deposited in Faraday Cup (mC)	First Filter Stage		Second Filter Stage		Third Filter Stage	
						Graphite[3] Filter Thickness (10^{-3} cm)	Transmitted[2] Charge (mC)	Graphite[3] Filter Thickness (10^{-3} cm)	Transmitted[2] Charge (mC)	Graphite[3] Filter Thickness (10^{-3} cm)	Transmitted[2] Charge (mC)
231	720	130	10.4	140	10.3	30 ± 1	7.1	33 ± 1	4.7	38 ± 1	2.1
251	720	130	10.1	130	10.4	51 ± 1	6.1	51 ± 1	2.3	51 ± 1	0

b. Calorimetry

Pulse	Peak[1] Acceleration Voltage (kV)	Peak[1] Diode Current (kA)	Energy[4] in Diode (kJ)	Average[5] Fluence (cal/cm^2)	Beam Energy Deposited in Calorimeter (kJ)
232	860	120	6.5	31 ± 6[6]	---[8]
239	670	140	6.7	13[7]	0.35
247	670	130	6.4	16[7]	0.42

NOTES:

1. Oscilloscope data
2. $\delta I\,dt$ error bars reflect truncation errors and errors associated in measuring small signals
3. Error bars reflect actual uncertainties and uncertainties associated with filter porosity
4. $\int V_{ACC} \cdot I_{DIODE}\,dt$
5. All calorimetry collected through 2.9 cm diameter aperture
6. Determined from all fully illuminated probes ± MSD
7. Calculated from deposited energy using 2.9 cm diameter
8. Not all of the beam was subtended by the calorimeter array

$$\phi = \frac{E}{A_k} * L \cong 39 \pm 4 \text{ cal/cm}^2$$

where

ϕ = fluence cal/cm^2

E = beam energy in diode: 1.6 kcal ± 10 percent

A_k = cathode area: 20 cm^2

L = lens ratio: 1/2

agrees reasonably well with the fluence calorimeter, 31±6 cal/cm^2.

*The fluence calorimetry and deposition profile calorimetry listed in Table 5 were collected on the Bonded Structures Program supported by AFRPL (under Contract No. F04611-74-C-0038).

SECTION IV

ANALYSIS

1. BEAM CHARACTERIZATION

The newly developed diagnostics functioned well throughout the program; i.e., they measured primary beam current as opposed to net current. This is shown by the qualitative and quantitative agreement between diode current waveforms and beam current waveforms shown in Figures 9 and 18, contrasted with the disagreement between diode current waveform and net current waveform shown in Figure 17.

a. Quantitative Beam Characterization Using the Multiply Internally Filtered Faraday Cup

The low dose testing described in Section III, Subsection 4, provided the data that were used to confirm that the multiply internally filtered Faraday cup could be used to characterize an electron beam. In this test sequence the total beam current deposited in the Faraday cup was virtually identical to the diode current (Figure 24). This suggested that beam transport efficiency was essentially 100 percent and that current loss due to backscattered electrons was negligible; i.e., albedo was suppressed for the magnetically transported beam (References 11 and 12). Therefore, the transmitted charge data were normalized by dividing total charge in the diode. The transmitted charge calculations were performed by either allowing backscattered electrons to escape (normal albedo) or by modifying the code to reverse the velocity vector of backscattered electrons (suppressed

albedo). The calculations were normalized by dividing transmitted charge by incident charge. The comparison of the data with calculated values shown in Figure 25 indicates that correlation is achieved with:

(1) 100 percent transport efficiency
(2) albedo suppressed
(3) 40^{o} to 50^{o} angle of incidence

In this test sequence the primary current monitor was not used so that conventional foil-stack deposition profile calorimeters could be used to measure the deposition profile for comparison with the deposition profile deduced from the transmitted charge data. The comparison of the measured deposition profile with calculated values is shown in Figure 26. The agreement is quite good for a 40^{o} angle of incidence but the 40^{o} to 50^{o} angle of incidence calculations certainly do not bracket the measured deposition profile as they did for the transmitted charge data. The deposition profile data were carefully inspected, revealing that the total energy deposited in the deposition profile calorimeter was only half of that deposited in a fluence calorimeter with a similar experimental geometry; i.e., through a 1-1/8 inch diameter, ¼ inch thick graphite aperture. It should be noted that this particular deposition profile calorimeter has been used successfully on OWL II (Reference 13); careful inspection of the OWL II data showed that beam energy deposited in the deposition profile calorimeter agreed with corresponding fluence calorimeter data.

The beam energy (hence fluence) calculated from diode voltage and diode current (or Faraday cup current) was about 20 percent higher than indicated by the fluence calorimeter. This is a reasonable agreement for the following reasons:

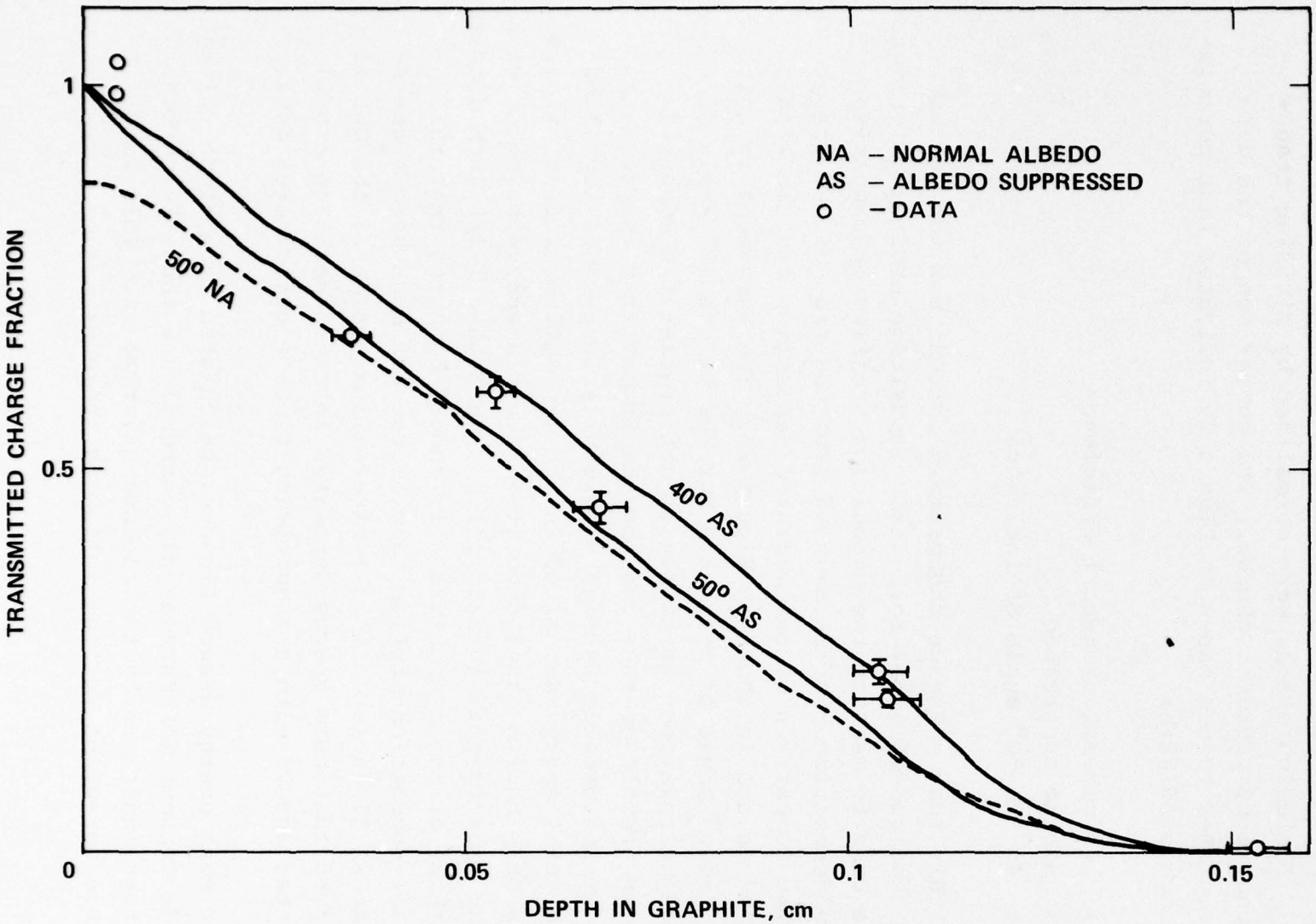

Figure 25 Comparison of measured transmitted charge with computed values, 1:2 beam expansion, 30 cal/cm^2 level.

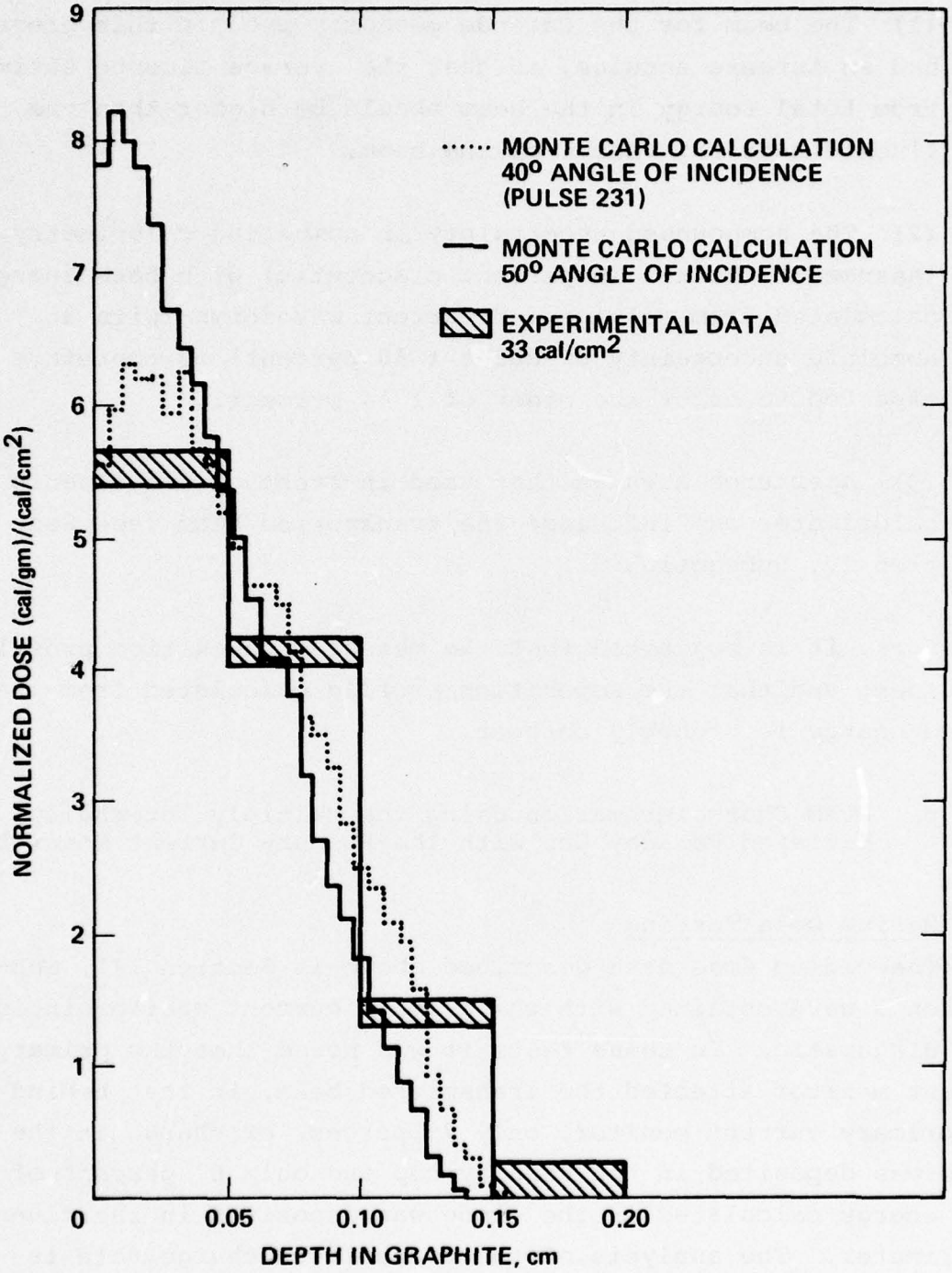

Figure 26 Comparison of the measured energy deposition profile in a thin foil calorimeter (pulse 247) and the computed profile based upon diode voltage and filtered Faraday cup data.

(1) The beam for the cathode geometry used in this program had an intense annulus, so that the average fluence estimated from total energy in the beam should be higher than the fluence near the center of the beam.

(2) The compounded uncertainty in comparing calorimetry (assumed to be a ± 10 percent diagnostic) with beam energy calculated from voltage and current waveforms (with an absolute uncertainty of about ± 10 percent) is therefore expected to be of the order of ± 14 percent.

(3) Apertures such as that used in front of the fluence calorimeter may influence the transported beam (see Section IV, Subsection 2).

Therefore, it is suggested that the measured deposition profile is suspect and that the deposition profile calculated from transmitted charge is probably correct.

b. Beam Characterization Using the Multiply Internally Filtered Faraday Cup with the Primary Current Monitor

Medium Dose Testing

The medium dose data described above in Section III, Subsection 3 were obtained with the primary current monitor included as a diagnostic. In these tests it was noted that the primary current monitor affected the transmitted beam, in that behind the primary current monitor, only 75 percent of charge in the diode was deposited in the Faraday cup and only 67 percent of beam energy calculated in the diode was deposited in the fluence calorimeter. The analysis of the transmitted charge data is further complicated by electron scattering by the materials of the primary current monitor, and the small change in magnetic

lens ratio between the primary current monitor and the Faraday cup. In an effort to account for the influence of the primary current monitor upon the transmitted charge data, the primary current monitor was treated in the analysis as an additional stage of filtering; i.e., all charge data were normalized by dividing measured charges by the charge in the diode; the charge transmitted through the primary current monitor was assigned an effective filter thickness (in graphite) corresponding to the areal density of half the thickness of foils in the primary current monitor (it is assumed that electrons that cross the vacuum barrier but are deposited in the remaining primary current monitor foils are measured as transmitted current by the primary current monitor); the filter depths for the Faraday cup data were increased by the areal density of the total foils in the primary current monitor. The resulting transmitted charge data are compared with calculated values in Figure 27.

The fluence calorimeter measurements obtained behind the primary current monitor, both with and without foils, can be used as transmitted fluence measurements. The beam energy deposited in the calorimeter was normalized by dividing by beam energy calculated in the diode. The results are shown in Figure 28, where the error bars (± 14 percent) represent the ± 10 percent combined uncertainties in the diagnostics. Comparison of transmitted charge data and transmitted fluence data with calculated values indicate reasonable correlation for:

(1) 100 percent transport efficiency
(2) albedo suppression
(3) 60° mean angle of incidence

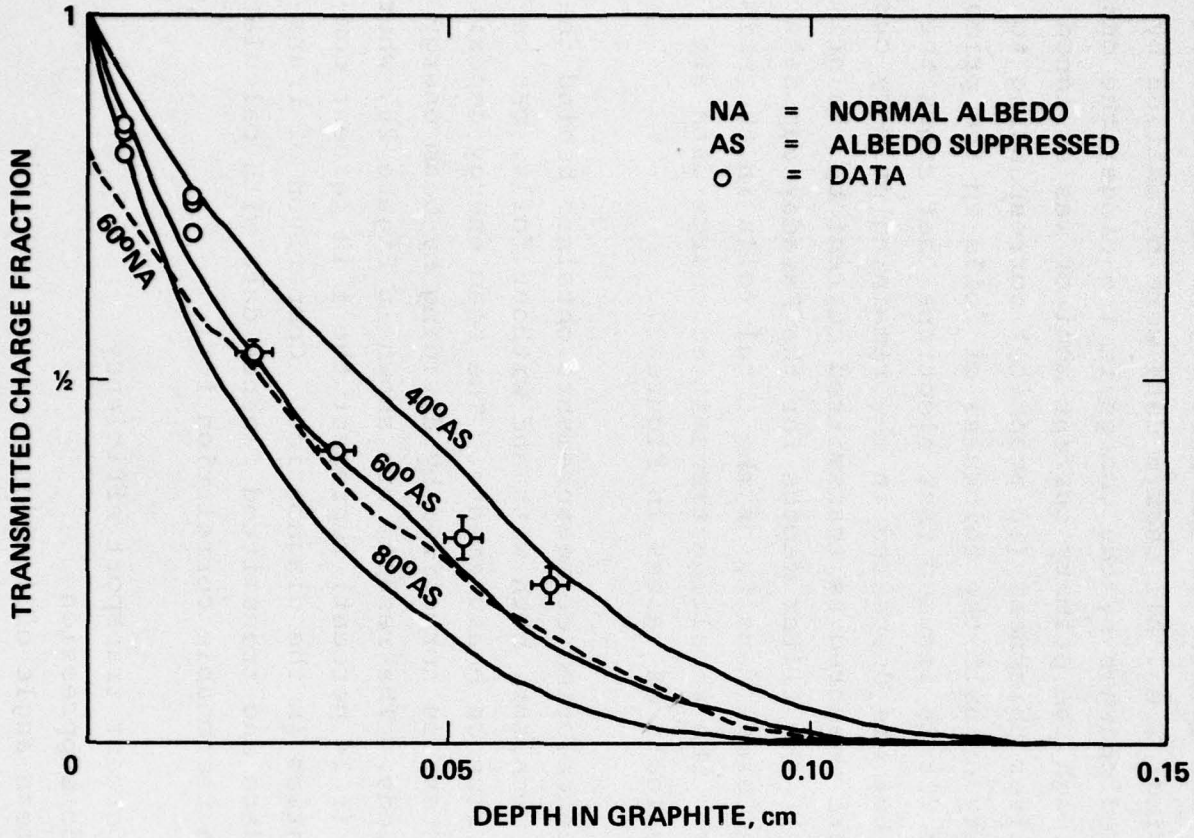

Figure 27 Comparison of measured transmitted change with computed values 2:1 beam compression 60 cal/cm^2 level.

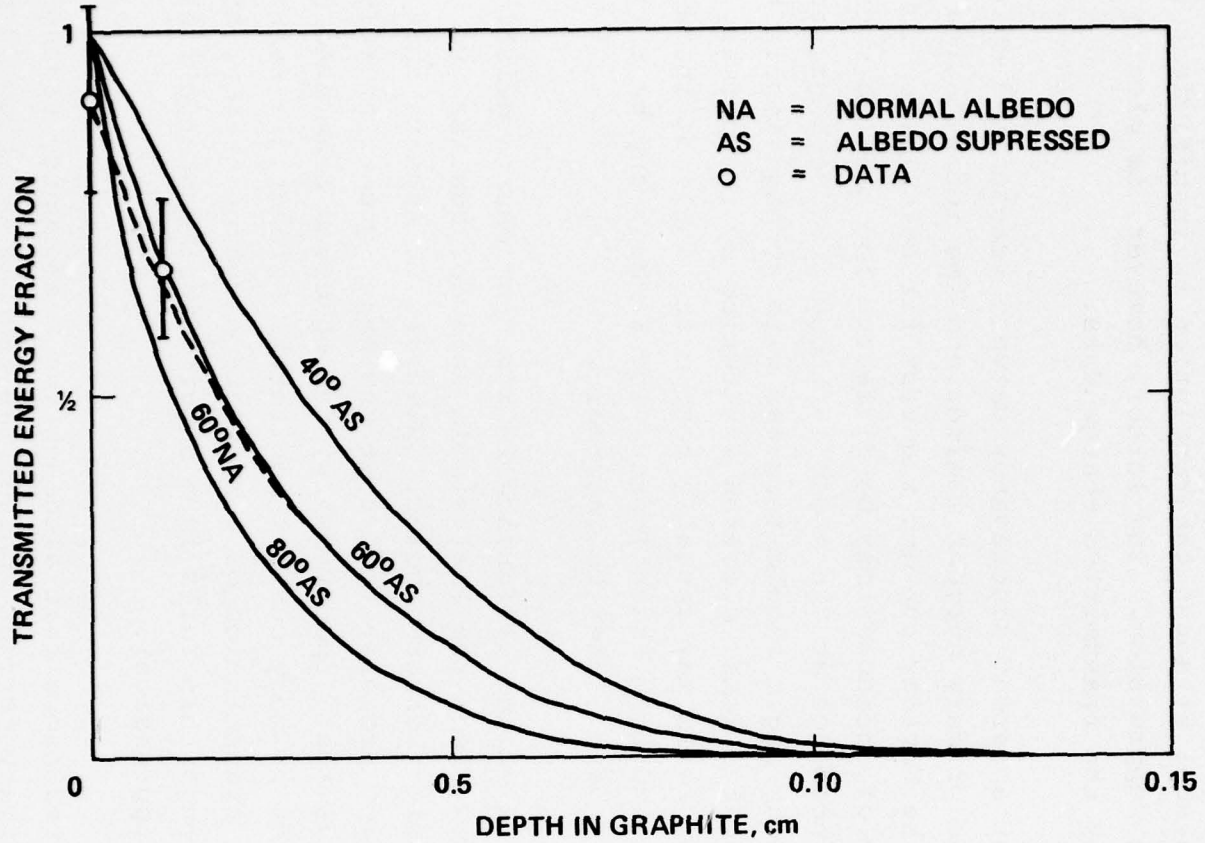

Figure 28 Comparison of measured transmitted energy with computed values 2:1 beam compression 60 cal/cm^2 level.

Despite the relatively large error bars on the transmitted fluence data, the fluence data serve to confirm the observed angle of incidence, although the resolution is insufficient to discern albedo suppression. The latter, however, is clearly demonstrated by the transmitted charge data.

The modest apparent discrepancy between transmitted charge measured by the primary current monitor and the total charge deposited in the Faraday cup and the best fit calculation suggests that the angle of incidence may be different for the two monitors. The angle of incidence at the anode is thought to be high, and although the mean angle should increase with propagation in the converging magnetic lens, electron scattering by the primary current monitor foils may actually reduce the angle of incidence of the transmitted beam which impacts the Faraday cup by making the transmitted beam closer to isotropic.

As a result of the difference in the beam characteristics at each monitor location, the analysis is somewhat qualitative and contains some minor discrepancies. However, it appears that the monitors function properly, and that the major questions relate to the beam dynamics. Specifically, the observed beam attenuation through the primary current monitor is evidently a natural consequence of transmission of a moderate electron energy, high angle beam through thin foils in a longitudinal magnetic field (with albedo suppression).

It was noted above that although the beam energy transmitted through the primary current monitor was reduced by about 33 percent, the fluence was reduced by only about 10 percent (when scaled by beam energy in the diode) and the fluence uniformity was somewhat improved by using the primary current monitor. This suggests that the intense annulus may be preferentially attenuated by the primary current monitor.

High Dose Testing

The high-dose data described in Section III Subsection 4 above, was also collected with the primary current monitor. In this test sequence the diode current was qualitatively different from beam current, Figure 20, because some of the diode current impacted the anode extension between the anode and the diode current monitor (I1). Since the injected beam current was not well defined, the primary current monitor was used to normalize the transmitted charge data in an effort to show that the multiply internally filtered Faraday cup could be used to characterize a high dose electron beam. Following the analysis in Section III, Subsection 4, transmission through the primary current monitor was calculated using 60-degree angle of incidence and albedo suppression. These calculations suggested that the charge transmitted through the primary current monitor was 90 percent of the charge measured by the monitor. Therefore the transmitted charge data were normalized by dividing by 90 percent of the primary current monitor charge. The calculations also indicated that the transmitted mean electron energy was degraded by 5 percent. Without exact information about the transmitted electron energy spectrum, calculations were made by scaling the diode voltage waveform. The transmitted charge data are compared with calculated values in Figure 29. Reasonable correlation is achieved for:

(1) 100 percent transport efficiency
(2) albedo suppression
(3) 80^{o} angle of incidence
(4) voltage degraded by 0 to 10 percent

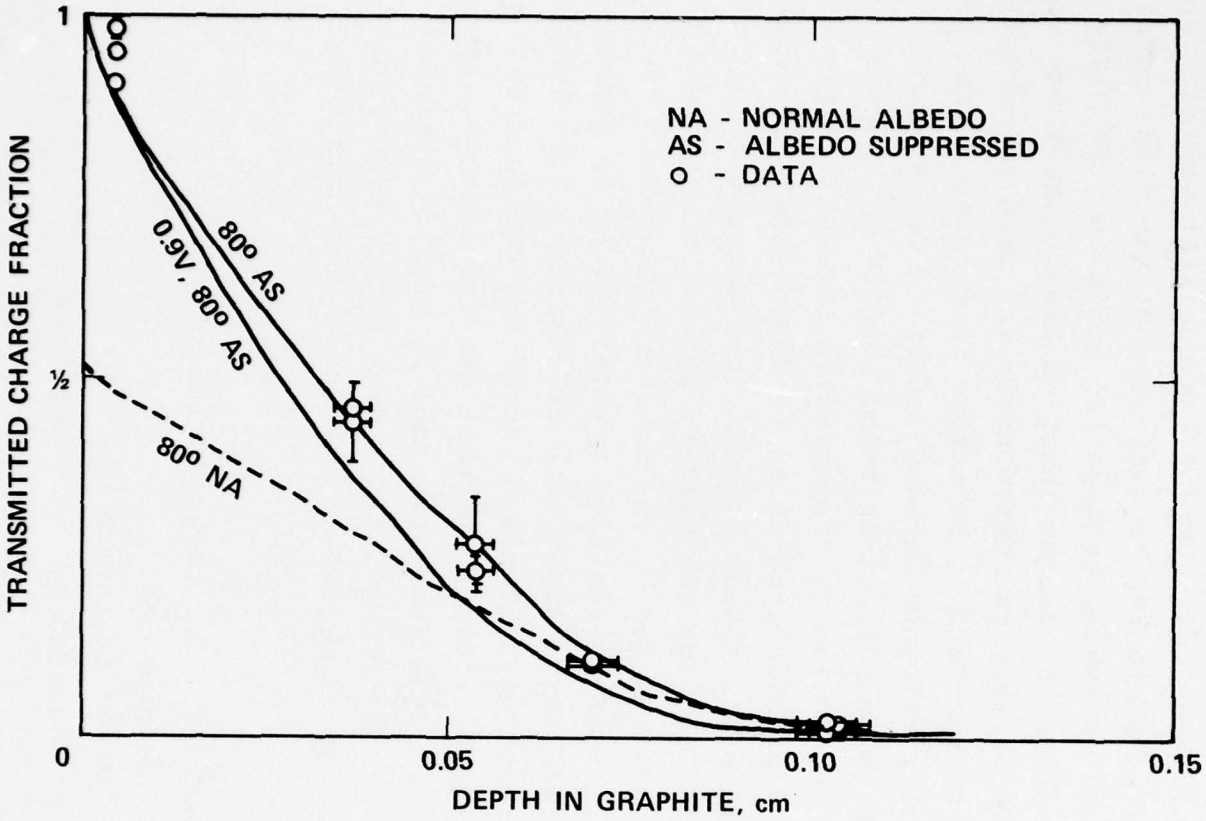

Figure 29 Comparison of measured transmitted charge with computed values 4:1 beam compression 225 cal/cm^2 level.

The normal albedo calculation is shown to indicate the significance of albedo suppression at very high angles of incidence.

The calculated electron beam energy deposition profiles are shown in Figure 30. These deposition profiles indicate that at high angles of incidence the deposition profiles are less sensitive than transmitted charge to the correlation parameters; in other words errors in determination of correlation parameters result in smaller errors in the quantity of concern.

On Pulse 212 the primary current monitor was located in the center of the lens near the Faraday cup. These data cannot be quantitatively analyzed since the diode current monitor data are inadequate. However, the raw data indicate that the total beam current was approximately 25 percent lower and that the transmitted charge deposition profile was representative of a much reduced angle of incidence. The results suggest that the primary current monitor functions properly at high dose, and that the angle of incidence was probably quite high at the primary current monitor, but is reduced by scattering in the primary current monitor before it enters the Faraday cup.

The analysis of the high-dose beam is again somewhat qualitative, but it demonstrates that the multiply internally filtered Faraday cup functions properly in that it can be used to investigate the characteristics of high dose electron beams.

2. APERTURES

Two sets of aperture data were collected in this program. The first set described in Section III, Subsection 2, utilized

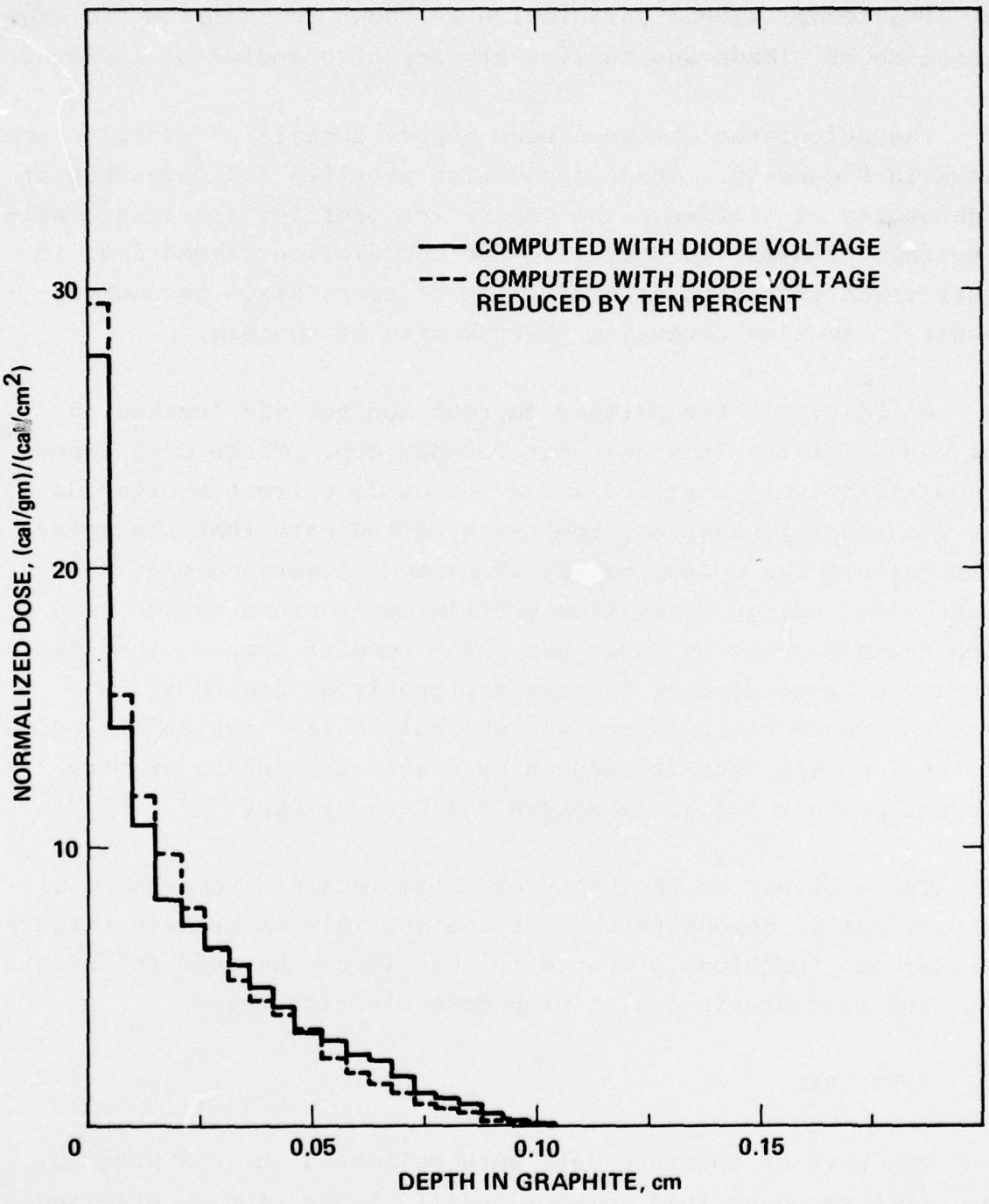

Figure 30 Comparison of computed deposition profiles for pulse 222 for 80-degree angle of incidence.

poor aspect ratio (0.32-cm, 0.64-cm and 1.3-cm-diameter, 0.25-cm-thick) graphite apertures. The data shown in Figure 11 are difficult to understand; the waveforms are qualitatively different from both diode current and each other. Scaling by the ratio of the aperture diameter to the beam area, the estimated charge deposited in the Faraday cup through the apertures is too high by a factor of 2 to 3. This is particularly disturbing because the 1.3-cm-diameter aperture was identical to the aperture used with one of the deposition profile calorimeters, which measured a fluence about half of that in a corresponding (unapertured) fluence calorimeter.

The second set of aperture data utilized high aspect ratios (0.64-cm- and 1.3-cm-diameter, 0.038-cm-thick) Ta apertures. The data shown in Figure 17 indicate some qualitative differences from beam current (primary current monitor), but the charge deposited in the Faraday cup is close to the expected value.

These observations indicate that either apertures perturb transported beams or the current density distribution varies with time. These effects must be understood before arrays of small internally filtered Faraday cups can be used to investigate deposition profiles across the target plane.

SECTION V

CONCLUSIONS AND RECOMMENDATIONS

Two new diagnostics for intense pulsed electron beams have been successfully developed and demonstrated. The first device, a Faraday cup with three internal filters, measures the total current deposited in the Faraday cup, and the current transmitted through each filter, providing data that can be used to establish the energy deposition profile. The second new diagnostic is a primary current monitor that measures the primary beam current (as opposed to the net beam current, which includes the plasma return current) in the region between the diode and the target. It provides data that determines the total beam energy (and hence the fluence) incident upon the target.

The Faraday cup with multiple internal filters has been shown to function properly at dose levels greater than 2000 cal/gm, and hence well above the limits for graphite calorimetry.

The primary current monitor performance has been demonstrated at moderate dose levels (~ 1000 cal/gm). The upper dose limit for operation of the primary current monitor was not clearly determined. The monitor was found to yield valuable cross correlation between the various beam diagnostics. It should also provide important information when test specimens are irradiated.

The use of the primary current monitor (in its present configuration) evidently perturbs the beam to an extent that varies with the beam environment. For a 500 to 600 keV beam at low

fluence levels, the mean energy and fluence of the transmitted beam were reduced on the order of 10 percent. At high fluence levels (with high mean angles of incidence) the transmitted fluence was substantially reduced. At higher beam voltages it is expected that the primary current monitor would introduce less perturbation of the beam. Moreover, it is possible that design modifications of the monitor could improve its performance for the beam conditions investigated in this study.

In addition to demonstrating the validity of the new diagnostics, several important characteristics of the beam and the supplementary diagnostics used during the evaluation tests were determined. First, for beams transported using longitudinal magnetic fields there have been several earlier experiments that could be explained only if electron albedo is suppressed; i.e., electrons scattered out the front surface of the irradiated target are reflected back in. Results obtained in this program provide convincing evidence of this phenomenon.

The data obtained for beam compressions of 2:1 and 4:1 and even for an expansion of 1:2 showed relatively high angles of incidence, which may be due in part to scattering introduced by the foils of the primary current monitor and perhaps also to the particular diode configuration used. The high angles of incidence, combined with the albedo suppression (albedo generally increases with the angle of incidence), leads to much higher peak dose levels than would be obtained for low angles of incidence and normal albedo.

A discrepancy in the results obtained with a deposition profile calorimeter was noted, even though the maximum energy deposition levels were moderate (~ 200 cal/gm). The depth dose data

were inconsistent with both the multiply filtered Faraday cup data, and fluence calorimeter data, while the latter two were nominally in agreement with each other. Since such depth-dose calorimeter data have been heavily relied upon in the past, this problem bears further investigation.

Potential problems with the behavior of beams passing into or through apertures or collimators were also indicated by some of the experimental results. An investigation of this phenomenon was beyond the scope of the present effort. However, work is needed on this problem to determine its magnitude and limits and to develop an understanding of the physics involved.

Finally, both during the performance of the experimental effort and the data reduction and analysis of the results, the benefits of ostensibly redundant, independent diagnostics were manifest. While multiplicity of the diagnostics reduced the rate at which data could be obtained, it greatly increased the value of the results, since it was frequently possible to eliminate ambiguities that would have otherwise remained.

REFERENCES

1. D. Pellinen, "A High Current, Subnanosecond Response Faraday Cup," Rev. Sci. Instr. 41, No. 9, 1347 (1970).

2. D. Pellinen, "A Segmented Faraday Cup to Measure MA/cm^2 Electron Beam Distributions," Rev. Sci. Instr. 43, 11, 1654-1658 (1972).

3. D. Pellinen and V. Staggs, "A Technique to Measure High Power Electron Beams," Rev. Sci. Instr. 44, No. 1 (1973).

4. W. C. Condit, D. Pellinen and D. Wood, "Current Density Measurements on Intense Relativistic Electron Beams," Bull. Am. Phys. Soc., 17, 11 (1972).

5. W. C. Condit and D. Pellinen, "Impedance and Spot Size Measurements on an Intense Relativistic Electron Beam Device," Phys. Rev. Letters 29, 263 (1972).

6. D. Pellinen, W. C. Condit, et al., "Generation and Diagnosis of Terawatt/cm^2 Electron Beams," submitted to Phys. Rev. Letters.

7. P. Spence, A. Lutze, and G. Yonas, "Generation, Control and Diagnosis of High Energy Density Electron Beams," PITR-205-1, Physics International Company, San Leandro, California (1969).

8. "Model 225-W Pulserad Operation and Maintenance Manual," Physics International Company, San Leandro, CA (1975).

9. H. Calvin and N. Bergstrom, "Computerized Data Reduction," PIIR 2-75, Physics International Company, San Leandro, CA., (1975).

10. J. Reaugh and L. Behrmann, "Documentation of Physics International Monte Carlo Electron Transport Computer Code," PIIR-9-71, Physics International Company, January (1971).

11. C. Stallings, K. Childers, and S. Shope, "High Dose Test Capability," PIFR-409, Physics International Company, San Leandro, CA (1973).

(References continued)

12. K. Childers and J. Shea, "Material Response Technology on Physics International Mylar Line," PIFR-423-1 and DNA 3448F, Physics International Company, San Leandro, CA. (1974).

13. K. Childers, V. Buck, and J. Shea, "Thermostructural Response of Cantilevered Titanium Alloy Beams Subject to Pulsed Radiation Heating," PIFR-836, Physics International Company, San Leandro, CA (1976).